Wastewater treatment plant design, plan and construction

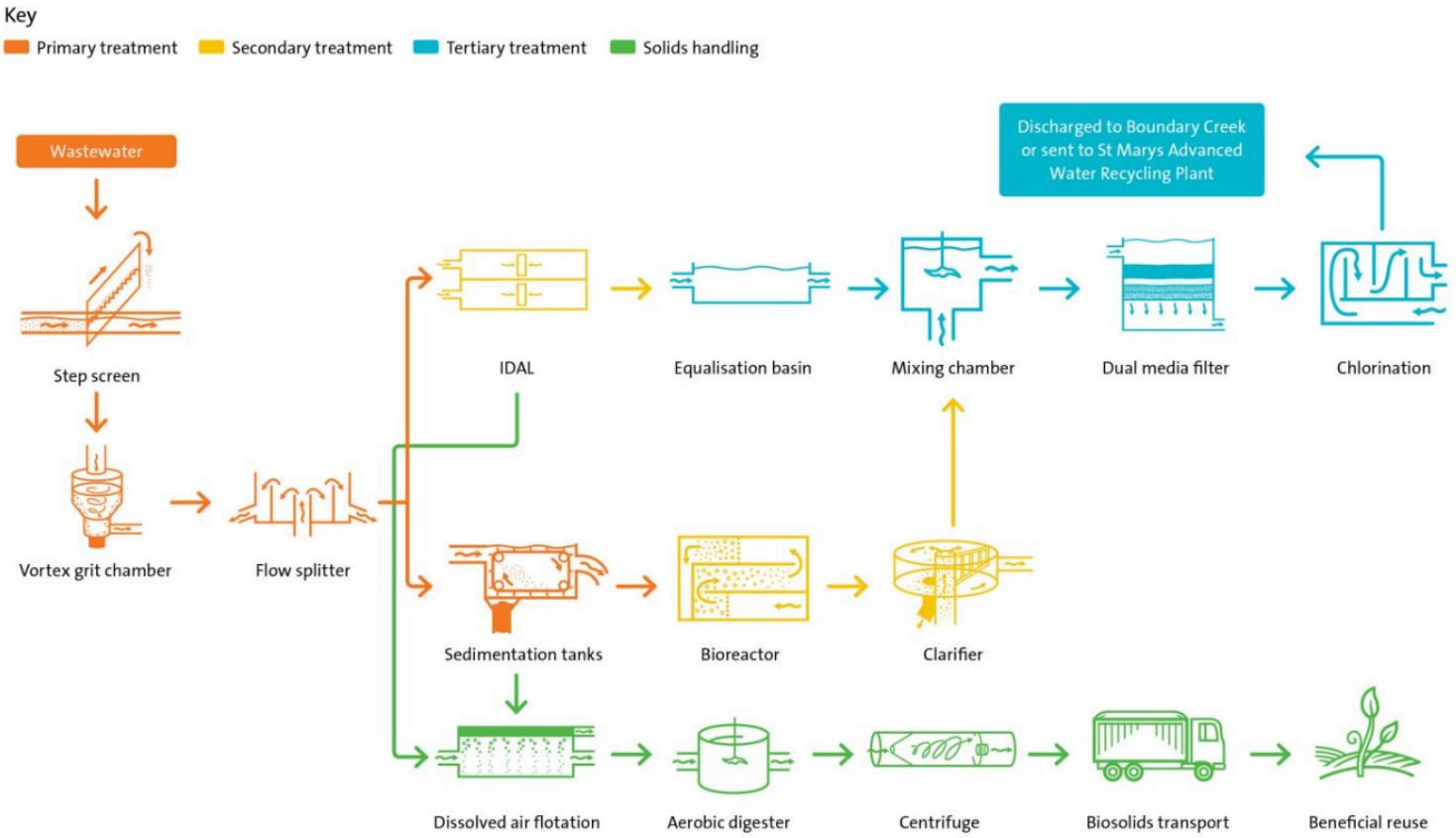

Figure 1: Steps illustrating wastewater treatment process (Source: https://www.sydneywater.com.au/) .

Abstract

A wastewater treatment plant comprises three treatment cycles. Although it may appear complex, it essentially involves separating solids from liquids through primary treatment, which includes a step screen to remove toilet paper, followed by a vortex grit chamber to extract heavy grits in order to achieve an adequate flow splitter. Human water waste proceeds to a sedimentation tank where heavy solids are transferred to tertiary treatment and liquids to the bioreactor and clarifier, as well as IDAL (Intermittently decanted aerated lagoons) for further clarification of the water, allowing solids to settle in the equalisation basin before passing through a mixing chamber and dual media filter for purification and subsequent disinfection via chlorination. The tertiary treatment of dissolved air flotation is more aerated through diffusion than the IDAL in order to sediment the solids, in contrast to the sludge cake, which is collected from the top of the dissolved air flotation tank. The sludge return is utilised in the aerobic digester as it is essential for the chemical reaction to remove or reduce the biomass

to dry centrifuge the solids for safe fertilisers. The following research acts as constructability advice for wastewater treatment utility.

Step Screening

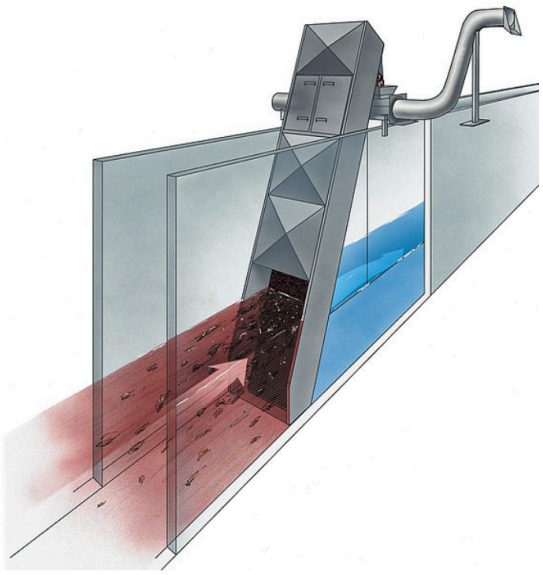

Figure 2: Simplified diagram of step screen

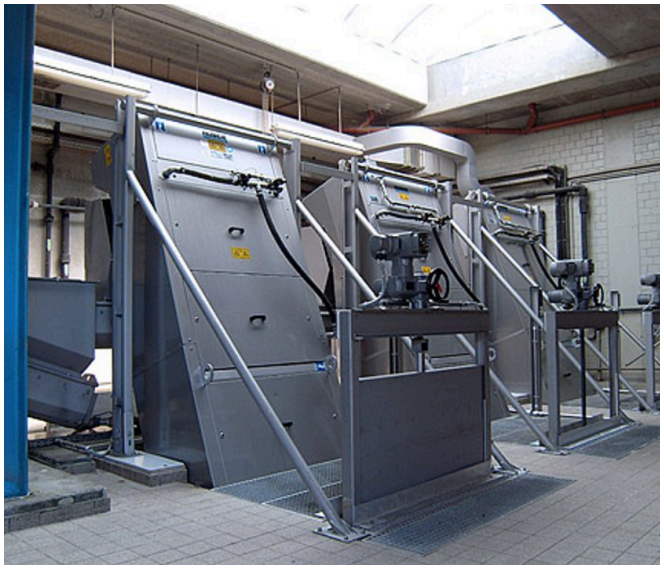

Figure 3:Actual step screen(Anon n.d.)

High separation efficiencies to remove non degradable objects floating from sewerage inlets at certain wastewater flow rate achieved with economical screening separation and transportation, the screens mechanically raises and collects non-biodegradable waste about 10 mm in diameter objects such as toilet paper.
The step system's functionality, user-friendly operation, self-cleaning effect based on countercurrent principle, ease of maintenance, capacity for extremely high screening volumes, and dependability under operation are all factors in its success and widespread adoption.

Grit Removal

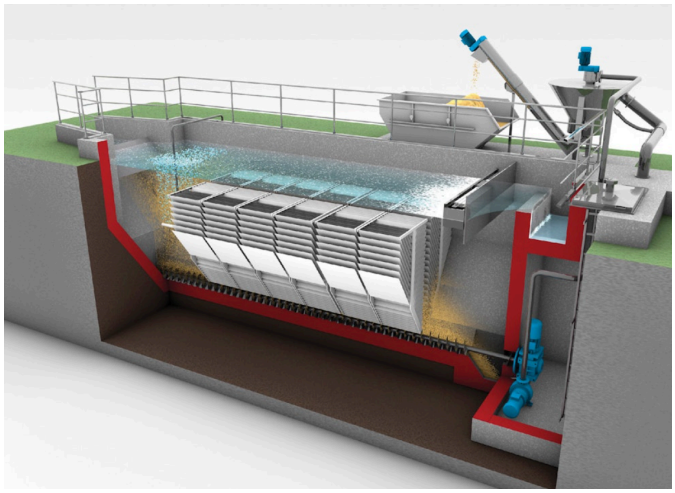

Figure 4: schematic sketch of grit collector (Operator 2019)

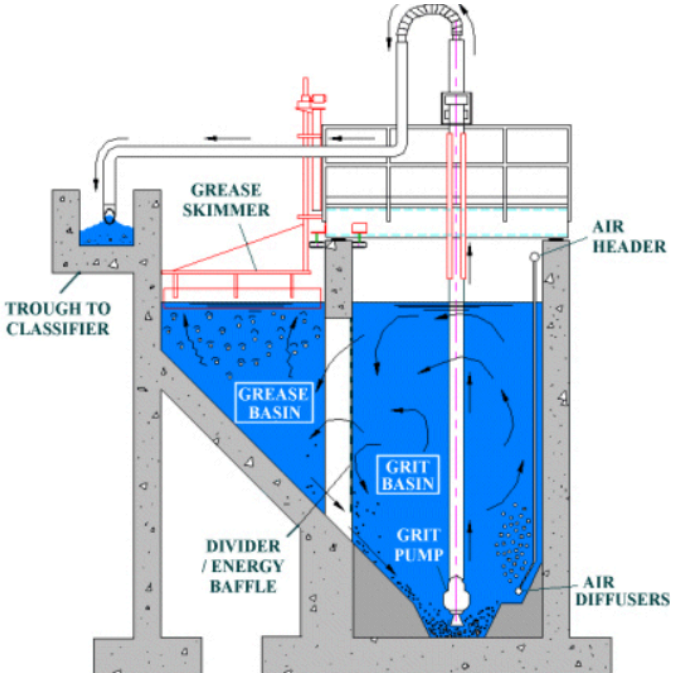

Figure 5: Cross section of grit collector through aerated chamber (Anon 2016)

An aerated chamber collects the Grit catch in a system, whereas an unaerated chamber uses a laminal separator to catch grit.

The design of vortex grit basins involves multiple parameters as shown in figure 6 that directly influence performance and operational efficiency. Key factors include floor slope, rotating impellers, grit hopper configuration, and inlet/outlet design. Each parameter contributes differently to the flow dynamics, grit removal efficiency, and maintenance requirements.

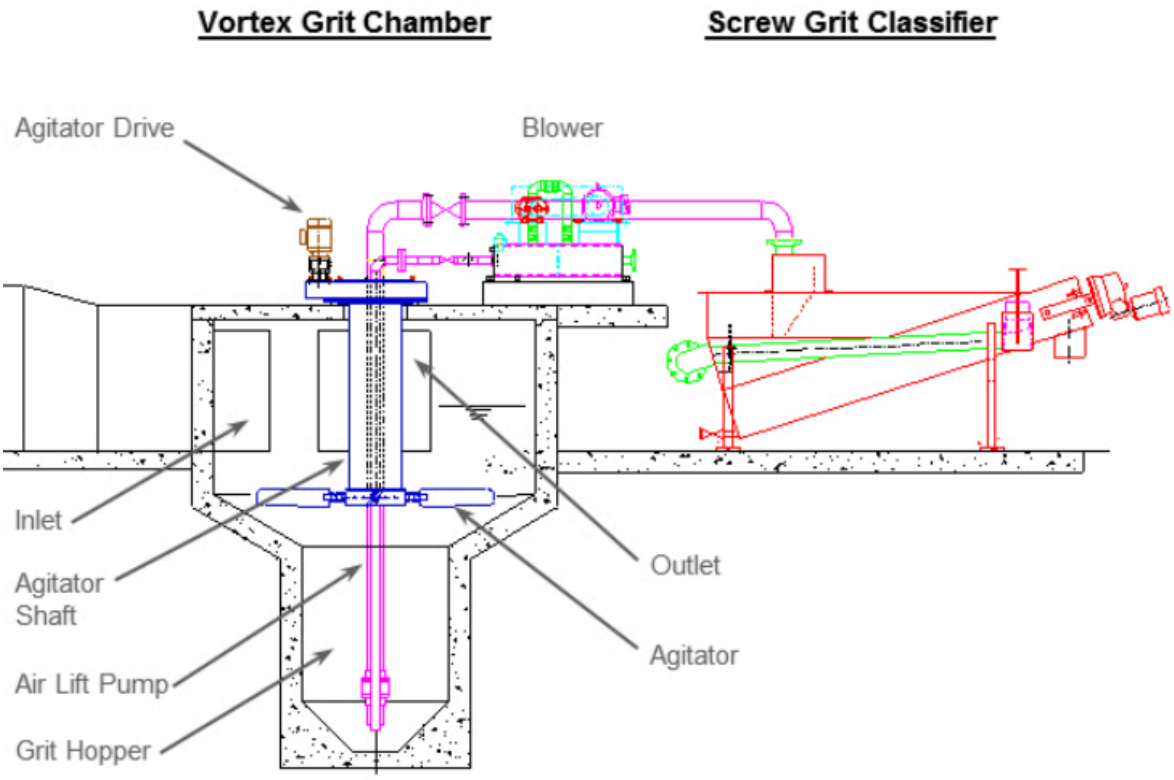

Figure 6 : CAD sketch of the vortex grit chamber (Anon n.d.).

1. Floor Slope

Floor slope plays a crucial role in determining the flow regime within the basin. A flat floor can induce a toroidal (doughnut-shaped) flow pattern, characterised by downward flow along the outer edges, inward movement along the floor, and upward flow at the centre. This pattern helps direct grit toward the centre for collection in the hopper. However, higher upward velocities associated with the toroidal flow increase the risk of grit particles being carried into the effluent, reducing removal efficiency.

Recent CFD (Computational Fluid Dynamics) analyses and field observations, such as those by Chien et al. (2010), show no consistent evidence of toroidal flow patterns in full-scale basins, especially with flat-floor designs. In fact, flat floors often lead to the accumulation of grit, particularly under low-flow conditions, which can later resuspend during peak flows and overload grit-handling systems. To address this, earlier experiments (e.g., APWA, 1974) involved converting flat floors to sloped floors to prevent such accumulation.

2. Rotating Impeller

Rotating impellers are conventionally used to maintain heavy organics in suspension while allowing finer grit to settle. However, settling velocities for organic solids and fine grit often overlap, which complicates the

optimization of impeller speed. One solution is to design the basin for optimal removal of grit based on particle size and density, supplemented by grit washing equipment to handle organics captured in the underflow.
CFD studies by (Chien et al. 2010)suggest that impellers may induce a reverse toroidal flow pattern in lab-scale basins, where flow moves outward along the floor and upward along the walls. This reverse pattern could inhibit effective grit capture. However, the impact of impellers on flow patterns diminishes in full-scale basins, where other design elements dominate flow behaviour.

3. Grit Hopper Design
A grit hopper provides a dedicated zone for settled grit to accumulate, isolated from the influent flow and impeller influences. However, grit accumulation in the hopper can cause blockages in the suction line of the grit pump, especially if intermittent pumping is employed. Proper design and operational strategies are essential to minimise these risks and maintain system reliability.
These design considerations highlight the complexity of vortex grit basin performance, emphasising the need for a balance between flow dynamics, grit removal efficiency, and maintenance. Analytical tools like CFD and empirical field studies provide valuable insights for optimising these systems.
Through the introduction of air along one side of the grit chamber, a spiral velocity pattern that is perpendicular to the flow through the tank is created. Lighter organic particles are suspended and eventually carried out of the tank, whereas heavier particles accelerate, diverge from the streamlines, and sink to the bottom of the tank. For the Removal of Grit While effluent exits the tank at the top, grit settles by gravity into the bottom of the tank (in a grit feeder). A grit pump or an air lift pump can be used to remove the grit that collects in the grit hopper. The procedure used to eliminate grit, silt, and sand from wastewater is called grit removal.

4. Numerical review over vortex operation

A study was conducted by (Pretorius 2012) and it mentioned that solid information on removal of grit in vortex grit basins is surprisingly rare owing to the difficulties in sampling and the low priority frequently set on the task. To find a common separation process in vortex grit basins, a review of full-scale and experimental plant data, mathematical models, and CFD model findings were conducted. The development of a model or equation for vortex grit basin design would result from the discovery of such a mechanism. Grit basin analysis demonstrates the absence of complex flow patterns and the insignificance of centrifugal forces. In vortex grit basins, the primary process for grit removal is sedimentation under the effect of gravity.

Table 1: Specific gravity of material that makes up grit

Material	*SG*	*Source*
Sand	1.52	(Lindeburg 2005)
Gravel	2.65	(Schmidt et al. 1997)
Quartz	2.64	(Incropera & DeWitt 1990)
Concrete	2.30	(Incropera & DeWitt 1990)

Cement	3.13	(Lindeburg 1999)
Aggregate	2.64	(Lindeburg 1999)
Eggshells	2.53	(Tsai et al. 2006)
Bone,rat	2.0-2.25	(Repo et al. 1988)
Coffee grounds (dry)	0.65	(Horio et al. 2009)

(Wilson et al. 2007)conducted a comparison between the theoretical velocities for SG = 2.65 and the settling velocities of collected grit. It was demonstrated that the larger grit particles (those larger than ~125 µm) sank at a nearly constant speed. The suggestion is that grit particles with a higher specific gravity, which settle more quickly than 125 µm "sand" particles (SG = 2.65), are not found in the effluent direction of wastewater treatment plants. Instead, they build up in the collecting system and are eventually removed at a peak flow event.

Since the early 20th century, vortex grit basins have been employed for removing grit from wastewater (Pretorius 2012). These basins serve dual purposes: as grit removal systems in wastewater treatment and as devices for separating suspended solids in combined sewer overflows.The consequences of inadequate grit removal include damage to downstream equipment and operational interruptions in downstream processing units, such as aeration basins and digesters.

Therefore, accurately evaluating the capacity of vortex grit basins is crucial for efficient plant operations. Vortex grit basins offer several benefits, including minimal power consumption, reduced odour potential (particularly when compared to aerated grit chambers), low head loss, and space efficiency. Consequently, these basins are often the preferred choice, especially for large-scale installations.

To calculate the terminal settling velocity of a grit particle, Stokes' Law is often used:

(1) $u_p = d_p^{\,2} g(\rho_p - \rho)/(18\mu)$

$u_p = terminal\ settling\ velocity\ of\ grid\ plate\ (m/s)$
$d_p = particle\ diameter\ (m)$
$g = acceleration\ due\ to\ gravity\ (9.8\ m/s^2)$
$\rho_p =$ *the particle density* (Kg/m^3)
$\rho =$ *fluid density* (Kg/m^3)
$\mu =$ *fluid viscosity* $(Kg/m.s)$

(2) $Re_p = \rho . u_p . d_p/\mu$

$Re_p = Reynolds\ number\ < 0.2$ *(Richardson et al. 2014)*
For $Re_p = Reynolds\ number\ > 0.2\ and\ 1,000$ *which applies for most grit particles*

(3) $u_p = d_p^{\,2} g(\rho_p - \rho)/\left(18\mu\left[1 + Re_p^{0.687}\right]\right)$

(4) $\eta = f(Q/d^n)$

$\eta = removal\ efficiency$
$Q = flow\ rate\ m^3/s\ or\ mgd$
$d = basin\ diameter\ in\ m$

(5) $Sf = s/S$

$Sf = sphericity$
s =surface area of a sphere having the same volume as the particle (m^2)
$S = Surface\ area\ of\ the\ particle\ (m^2)$

(6) $\eta = \frac{1-\phi exp[\alpha(\phi-1)]}{\frac{1}{\phi}-\phi exp[\alpha(\phi-1)]}$

$\phi = u_p/SOR$ the ratio of terminal grit particle settling velocity to surface overflow rate
$R = Volumetric\ ratio\ of\ underflow\ to\ influent\ flow$
$\alpha = 54\ pelect\ number$ the tangential velocity at the edge of the basin, which seems to be observed and differs from the inflow velocity. A non-measurable approach to α prediction would be necessary for a designer.
The system is highly mixed and turbulent when α = 0, which leads to a high removal efficiency, find equation (7)

(7) $\eta = \phi(\phi + 1)$

(8) $\eta = \phi$

In a vortex basin, the two extremes are represented by equations 7 and 8. When analysing main clarifiers and taking discrete particle settling into account, equation 8 is occasionally utilised.

(9) $\phi = \eta(1 - \eta)$

(10) $SOR = u_p(1 - \eta)/\eta$

$SOR = surface\ flow\ rate\ (m/h)$

(11) $Q_p = Q_m(\eta L_r^2 + 0.75[1 - \eta]L_r^{2.5}$

$Q_p = prototype\ flow\ model\ (L/s)$
$Q_m = model\ flow\ (L/s)$
$L_r = Length\ ratio$ prototype chamber diameter/ model chamber diameter

Tabel 2: Reference of η values for calculation

Values of η to obtain	
2	This suggests that the primary mechanism for removal in a vortex grit basin is gravity sedimentation. The ratio Q/d2 would be analogous to the surface overflow rate (SOR), which would serve as a crucial design parameter.

2.5	Based on their consistent Froude number, early workers seem to have embraced this as the proper value.Applied to free-surface flows, the primary effect is Froude number, which also guides similarity rules for such flows (White 1994)The Froude number can be defined as the ratio of gravity to inertia, to put it simply. It has been used since the beginning to analyse vortex grit basins (Pretorius 2012).
3	Unit volume and HRT would be equivalent to d^3. HRT is mentioned in certain removal efficiency theories for sedimentation basins, notably in relation to rectangular basins. This would be an unexpected outcome.

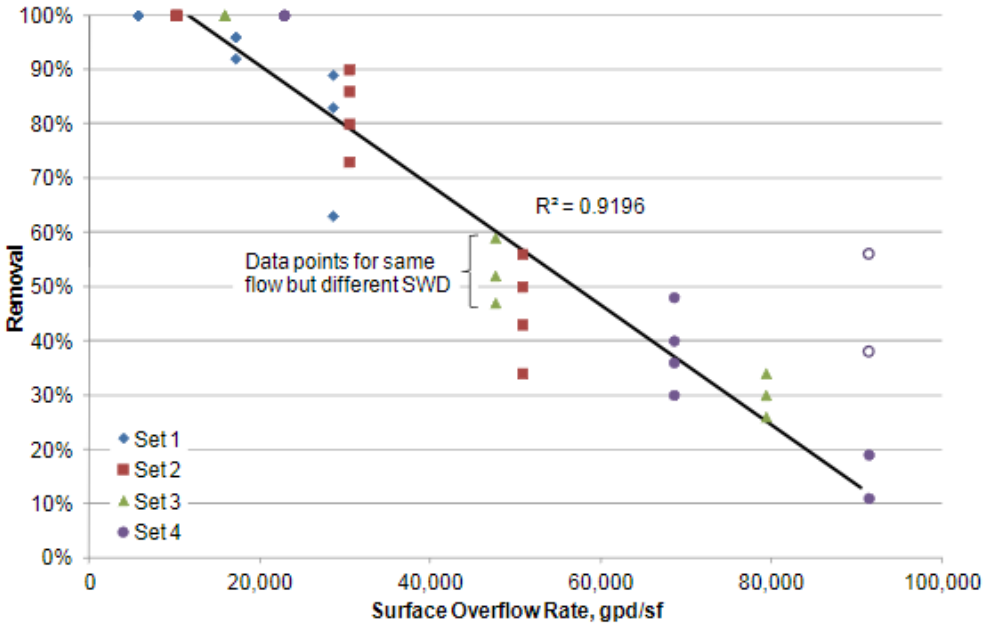

Figure 7 : Removal with respect to SOR (Sullivan et al. 1974)

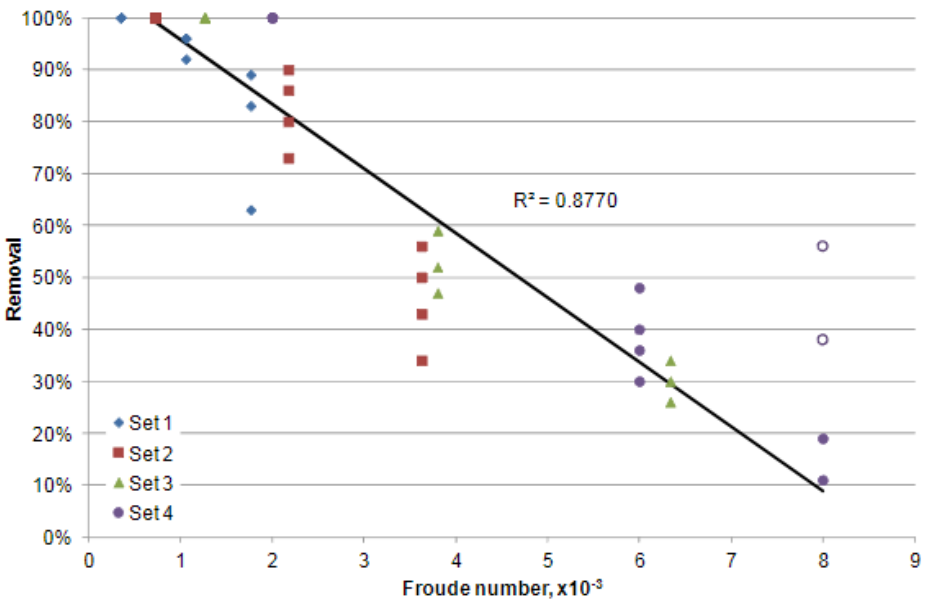

Figure 8 : Removal with respect to Fr (Sullivan et al. 1974)

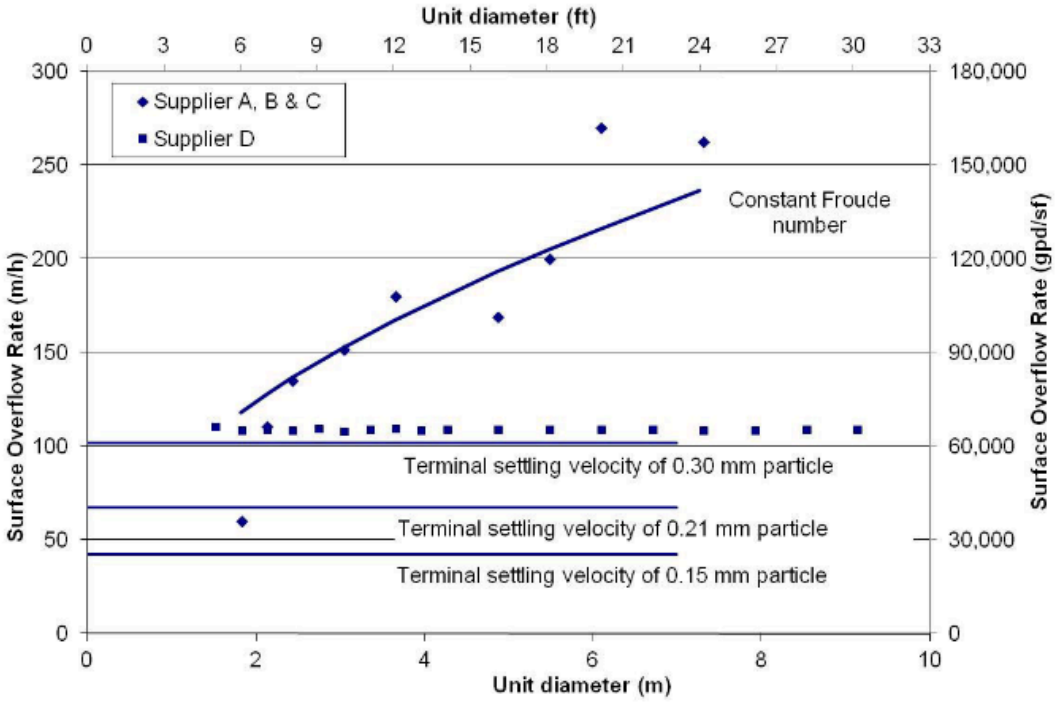

Figure 9: Particle Terminal Settling Velocities and Vortex Basin Design Capabilities

The relationship between removals and surface overflow rate (SOR) is clearly demonstrated in Figure 9 above, exhibiting a strong correlation. Variations in removal at each tested flow (SOR) are observed due to differing liquid depths, suggesting that deeper liquid levels may enhance removal within the tested range. The ratio of SWD to liquid depth ranged from 0.3 to 0.9, whilst in current full-scale designs, this ratio typically falls between 0.4 and 0.65.

Given the fixed diameter of the test unit, it was not possible to determine whether liquid depth or hydraulic retention time (HRT) had a greater influence on removal, as these parameters were directly proportional in this setup. All experiments were conducted in a unit with a sloped floor, precluding verification of any benefits from the cone volume.The unexpectedly high removals at elevated SOR, represented by two hollow data points on the right, indicate that the unit may have achieved increased removal through centrifugal separation. However, this phenomenon is unlikely to occur in full-scale vortex units due to low inlet velocity (and head loss), larger unit radius, and the use of peripheral outlets.

The researchers propose that the optimal design could have an α value as high as 1.5. Utilising this figure 9, the safety factor for 90% removal is 1.7, whilst for 95% it is 2.1. This indicates that a more precise estimation of α is crucial for practical designs. Two approaches could achieve this: firstly, developing an analytical solution that expresses α in terms of variables known to the designer; secondly, determining α experimentally and applying it to similar designs.

The researchers seem to suggest that α would remain constant if the ratio between surface overflow rate and inlet velocity is maintained. Current vortex grit basin designs typically aim to keep inlet velocity constant, based on the estimated velocity needed to suspend coarse grit. Consequently, sizing vortex grit basins to maintain a constant surface overflow rate would preserve a constant α value, ensuring consistent performance across differently sized basins with constant inlet velocity and SOR.

The researchers' modelling and experimental testing revealed that tank diameter (surface overflow rate), inlet diameter (inlet velocity), and outlet geometry were the three most influential parameters on performance. The impact of the latter two will be discussed subsequently.

A study conducted by (Chien et al. 2010) examined a vortex grit basin's failure to meet specified removal efficiency. Their CFD model indicated that halving the flow through the basin from 70 to 35 mgd, thus reducing surface overflow rate by 50%, would decrease the maximum velocity from 6 to 2 ft/s. Furthermore, the model predicted an increase in coarse grit (diameter = 649 µm; SG = 1.4) removal from 89% to 100%, and medium grit (diameter = 254 µm; SG = 1.4) removal from 7% to 72%. However, within two years of commissioning the vortex grit basins, the plant had to halt downstream aeration basins to remove grit for the first time ever. Grit was also discovered in secondary clarifiers and chlorine contact basins.

The figure 9 also shows the typical settling velocities for different particle sizes that are utilised in grit removal standards. It should be noted that the terminal settling velocities were calculated with the optimistic assumption of an SG of 2.65, as supported by the data in Table 1.

The figure indicates that, under the most advantageous set of assumptions, i.e., SG = 2.65 and that equation 8 is correct, even the most conservative of the suppliers would only achieve partial removal of the three particle sizes indicated. According to the statistics, most suppliers of big vortex grit basins are overly enthusiastic about their capability.

Flow Splitter

Wastewater is sent to various treatment stages using flow splitters, which maximises treatment efficiency and ensures proper loading on each unit. The research topic will investigate the hydrodynamic performance of hydraulic structures, focusing on flow-induced vibrations, sediment transport, and water level dynamics. (Steven J. Wright, Daniel B. Schlapfer, Razik Al-Saigh 1988) study will analyse the negligible impact of vortex shedding on vane structures, with vibration frequencies exceeding 65 Hz compared to a maximum shedding frequency of 0.15 Hz. Additionally, it will assess sedimentation patterns in splitter chambers under varying flow regimes and grit characteristics, identifying the impact of increased plant flows on sediment deposition. The study will also examine water surface level variations across overflow weirs, correlating them with flow distribution patterns to optimise sensor placement and minimise deposition zones.

Numerical review of split chamber

Design practice example (Caltrans Division of Design 2020)

This design example outlines the installation of an Upstream Flow Splitter (UFS) upstream of a Best Management Practice (BMP) Infiltration Basin at a site in Orange County. The basin's bottom elevation is set at 52.43 metres to maintain a 3.05-meter clearance above the seasonally high groundwater level of 49.38 metres. With an infiltration rate of 25.4 mm per hour for the sandy loam soil and a safety factor of 2, the water quality volume (WQV) depth in the basin is limited to 0.61 metres to achieve a 48-hour drawdown period. As a result, the water surface elevation for the WQV (WSWQ) is set at 53.04 metres.

The basin operates "offline" by using a UFS to regulate inflow, ensuring that the maximum 25-year water surface elevation in a surcharged condition (WSSUR) stays at least 0.21 metres below the roadway subgrade. The allowable WSSUR elevation is limited to 53.09 metres. The UFS control depends on the storage volume within the downstream BMP. Figures 10, 11, and 9 provide schematics and profiles of the storm drain, UFS, and BMP Infiltration Basin. The discharge from the BMP will flow into Orange County Creek, which runs adjacent to the project site.

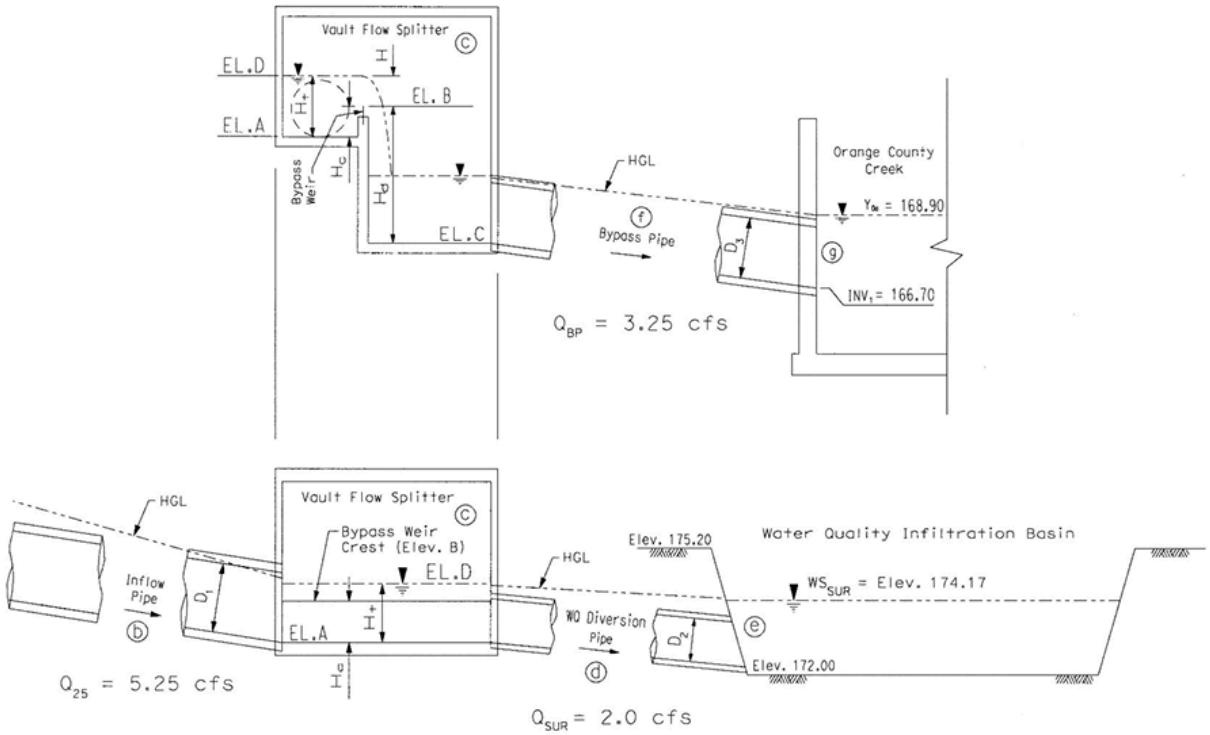

Figure 10: System Profile Showing Flow in the Surcharged Condition

This design example in figure 10 outlines the installation of an Upstream Flow Splitter (UFS) upstream of a BMP Infiltration Basin at a site in Orange County. The bottom of the basin is set at 52.43 metres to maintain a 3.05-meter clearance above the seasonally high groundwater level of 49.38 metres. The infiltration rate of the sandy loam soil is 25.4 mm per hour. With a safety factor of 2, the depth of the Water Quality Volume (WQV) in the basin is limited to 0.61 metres to achieve a 48-hour drawdown. As a result, the WQV water surface elevation (WSWQ) is set at 53.04 metres.

The basin is designed "offline," with a UFS regulating inflow to ensure the maximum 25-year water surface elevation under surcharged conditions (WSSUR) remains at least 0.21 metres below the roadway subgrade. The allowable WSSUR elevation is set to 53.09 metres. UFS control is based on the volume stored in the downstream BMP. Figures 8-3, 8-4, and 8-2 provide schematics and profiles of the storm drain, UFS, and BMP. The BMP will discharge into Orange County Creek, which flows adjacent to the site.

Given Data

The following hydrologic data and design parameters inform the UFS design:

- Q25 = 0.149 m^3/s (Peak design flow rate for the storm drain system)

- TC = 15 minutes
- WQV = 481 m^3 (Water quality volume for treatment)
- WSWQ = 53.04 m
- WSSUR = 53.09 m (Maximum water surface elevation under 25-year peak flow)
- QSUR = 0.057 m^3/s (Maximum discharge from the overflow structure)
- VX = 0.054 acre-ft = 66 m^3 (Flow volume at 50% of Q25 over 15 minutes)
- WSX = 52.58 m (Pool elevation for VX)

Additional Design Parameters

- BP Pipe Invert Elevation at Orange Creek (INV1) = 50.82 m
- Bottom Elevation of BMP Infiltration Basin (INV2) = 52.43 m
- TOG Elevation on Drainage Inlet Upstream of UFS = 54.48 m
- IN Pipe Diameter (D1) = 0.61 m

Step 1: Select the Diameter of the WQ Diversion Pipe and Set the Bypass Control Elevation (BCE)

The proposed UFS location is selected with a WQ diversion pipe length of approximately 9.14 metres. The BCE is set at 53.04 metres, matching the WSWQ.

- BCE = WSWQ = 53.04 m
- Initial Invert Elevation of WQ Diversion Pipe (Elevation A) = 52.58 m

To minimise headwater depth on the WQ diversion pipe at Q25, the largest standard pipe diameter of 0.46 metres is chosen. Hydraulic analysis using HY-8 (FHWA, 2016) confirms that the selected 0.46-meter pipe will maintain the headwater depth below the BCE at Q25.

Hydraulic Analysis Parameters

- Q25 = 0.149 m^3/s
- Pipe Diameter = 0.46 m
- Pipe Length = 9.14 m
- Upstream Invert Elevation = 52.58 m
- Downstream Invert Elevation = 52.43 m
- Slope = 0.0167 m/m
- Manning's "n" = 0.012 (Precast RCP)

The hydraulic analysis, summarised in Table , indicates that the peak flow rate of 0.149 m^3/s is low relative to the UFC's cross-sectional area, resulting in a flow velocity below 0.3 m/s. As the velocity head is negligible, it is not included in the calculation of headwater depth.

Table 3: Rating table for WQ diversion pipe

Flow rate m^3/s	**WQ Diversion Pipe Headwater depth (m)**

0	0
0.0014	0.0182
0.0297	0.1584
0.0447	0.1851
0.0594	0.2286
0.0891	0.2956
0.1042	0.3231
0.1189	0.3535
0.1339	0.3779
0.1486	0.4053

The velocity for half-full flow and an empty basin is checked to ensure a minimum self-cleansing velocity of 0.91 m/s during smaller storm events. The minimum pipe slopes required to achieve this velocity are provided in Table 8-2 and must meet the standards outlined in HDM Topic 838.4(3).

- Manning's "n" = 0.012 (for precast RCP, per HDM Table 851.2)
- Minimum Velocity (v) for half-full flow = 0.91 m/s

Table 4: Half Full Flow Hydraulic Analysis of WQ Diversion Pipe

Pipe Diameter (D)(m)	Pipe Area $A = \frac{\Pi D^2}{4}$	Half Full Area a=A/2 m^2	Half Full discharge Q=Va=3a m^3/s	Wetted Perimeter, $\rho = \frac{\pi D}{2}$ m^2	Hydraulic Radius $R = a/p$ m^2	Minimum Allowable slope S
0.457	0.538	0.269	0.075	0.718	0.114	0.0021

The velocity for half-full flow and an empty basin is checked to ensure a minimum self-cleansing velocity of 0.91 m/s during smaller storm events. The minimum pipe slopes required to maintain this velocity are provided in Table 3. These slopes must meet the requirements of the HDM

- Manning's "n" = 0.012 (for precast RCP, per HDM Table 851.2)
- Minimum Velocity (v) for half-full flow = 0.91 m/s

The slope of the WQ diversion pipe (0.0167 m/m) exceeds the minimum required for half-full flow, ensuring the pipe is self-cleansing, and the proposed pipe profile is acceptable.

Step 2: Calculate Dimension "Hc"

Dimension **Hc** is calculated as:

$$H_c = Elevation\ B - Elevation\ A = 53.04 - 52.58 = 0.46\ m$$

The hydraulic profile for the QHDM and a tailwater at WSX is shown in Figure 11.

Step 3: Calculate the Maximum Allowable Water Surface in the UFS During Bypass and the Corresponding Hydraulic Head "H"

The maximum allowable water surface elevation in the Infiltration Basin during surcharge (WSSUR) is 53.09 m, with a surcharge flow rate (QSUR) of 0.057 m³/s. The head loss through the WQ diversion pipe for QSUR is added to WSSUR to determine the maximum allowable water surface elevation in the UFS and the corresponding hydraulic head H for the bypass component (see Table 8-3

Table 5: Full Flow Hydraulic Analysis of WQ Diversion Pipe (QSUR)

Pipe Diameter (D)(m)	Pipe Area $A = \frac{\Pi D^2}{4}$	Velocity V=Q/A (m/s)	Velocity Head $V_h = V^2/2g$	Entrance Loss $0.2V_h$	Exit Loss $1.V_h$	Friction slope SF (m/m)	Friction Head Loss HT Hf = SfL	Total Head Loss HT (m)
0.457	0.538	0.344	0.269	0.075	0.718	0.114	0.0021	0.0101

Entrance loss coefficient (Ke) = 0.2, for rounded headwall entrance (FHWA 2009). Exit loss coefficient (Ke) = 1.0, for exit with D2/D1 > 10 and V < 2.0 fps (FHWA 2009). Sf = [Qn/(KQD2.67)]2, KQ = 0.46 in English units (FHWA 2009).

Step 4: Calculate Elevation D and the Hydraulic Head H

$$Elevation\ D = WS_{sur} + H_T = 53.09 + 0.0101 = 53.1\ m$$

$$H = Elevation\ D - Elevation\ B = 53.1 - 53.04 = 0.06$$

The hydraulic profile for the bypass/surcharge condition is illustrated in Figure 9.

Step 5: Determine the Size of the Bypass (Weir Length or Pipe Diameter) and Select the Type of UFS

The bypass flow rate for the UFS design is calculated by subtracting the surcharge flow through the Infiltration Basin (which passes over the basin's overflow structure) from the peak flow rate:

$$Q_{BP} = Q_{HDM} - Q_{SUR} = 0.149 - 0.057 = 0.092\ m^3/s$$

If a **Type 4 UFS** is used, the BP pipe must convey 0.092 m³/s with only 0.06 m of headwater. Rating curves for various BP pipe diameters are shown in Figure 8-1.

It is observed that a headwater depth of **0.06 m** on a Type 4 BP pipe, with diameters of **600 mm** or **900 mm**, results in a bypass capacity of less than **0.0085 m³/s**, which is far below the required **0.092 m³/s**. Achieving the necessary bypass flow would require raising the headwater elevation in the UFS to more than **53.29 m**, exceeding both the **QSUR** and **WSSUR** limits in the Infiltration Basin. As this conflicts with the BMP design criteria for the site, the Type 4 UFS is unsuitable, and a weir-type UFS is proposed.

Weir Length Calculation

The weir equation is used to determine the required weir length. The coefficient for an submerged sharp-crested weir (**CSCW**) is calculated as:

$$C_{scw} = 3.27 + 0.4(H/H_c) = 3.27 + 0.4(0.06/0.46) = 3.32$$

The required weir length (**Lw**) for a sharp-crested weir with end contractions is calculated for **Qw = QBP**:

$$L_w = \left[\frac{Q_w}{CSCW \times H^{1.5}}\right] + 0.2H = \left[\frac{0.092}{3.32 \times 0.06^{1.5}}\right] + 0.02(0.06) = 3.35\ m$$

To accommodate this weir length, a **Type 1 UFS** is selected for the site.

Step 6: Set the Invert Elevation for the BP Pipe and Calculate Hydraulic Head (Hd)

Since the flow rate over the weir is **0.092 m³/s**, a hydraulic analysis of the BP pipe is performed using the given tailwater conditions to finalise the invert elevation and hydraulic head.

The elevation at Orange County Creek is 51.48 m, and the invert of the BP pipe where it connects to the creek is set at 50.81 m. For the initial analysis, the invert elevation of the BP pipe (Elevation C in Figure 8-6) is set at 52.27 m. The hydraulic analysis must confirm that the pipe profile provides a minimum 250 mm of freeboard to the weir crest (BCE).

The analysis is performed using HY-8 and is based on the following parameters:

- Flow rate (QBP) = 0.092 m³/s
- Diameter = 600 mm (Same as IN pipe diameter)
- Pipe length = 25.91 m
- Upstream invert elevation (Assumed) = 52.27 m
- Downstream invert elevation = 50.81 m
- Slope = 0.0565 m/m
- Manning's n = 0.012 (for precast RCP)

The results of the hydraulic analysis are summarised in Table 8-4. This analysis ensures the proposed pipe profile can convey the required flow while maintaining adequate freeboard and preventing overflow.

Table 6: Rating Table for BP Pipe

Flow rate m^3/s	WQ Diversion Pipe Headwater depth (m)
0	0
0.0014	0.015
0.0184	0.106
0.0277	0.134
0.0036	0.155
0.046	0.176
0.055	0.192
0.064	0.207
0.073	0.225
0.082	0.24
0.0911	0.252 EL. 52.52

Elevation C = 52.27 m

$H_d = Elevation\ B - Elevation\ C = 53.04 - 52.27 = 0.77$

The hydraulic profile for this analysis is illustrated in **Figure 11**.

Step 7: Confirm UFS Fits within Vertical Drop Available

The system profiles for the WQ flow path and bypass flow path are illustrated in **Figures 12** and **11**. The designer confirmed that there is adequate vertical drop to accommodate these profiles and that the UFS fits beneath the proposed finished grade at the site.

Step 8: Complete Hydraulic Analysis for Upstream Drainage System

A hydraulic analysis for the peak design flow rate (Q_{525}) was conducted for the upstream drainage system using a downstream water surface control equal to the maximum water surface elevation in the UFS, calculated in Step 3. This surface was set at 53.08 m (174.20 ft). The resulting hydraulic grade line (HGL) provided sufficient freeboard at all drainage inlets, confirming that the UFS design is acceptable.

Table 7: Design summary of the flow splitter.

Design Summary	Metres
WQ Diversion pipe diameter	0.457
UFS Type	Type 1
Length Bypass Weri (Lw)	3.34
HcType1	0.45
3.34Hd	0.762
Elevation A	52.57
Elevation B (BCE)	53.03
Elevation C	52.27

The UFS in this example effectively directs the required water quality volume (WQV) to the proposed BMP Infiltration Basin. The WQ diversion pipe meets the conveyance requirements for the peak design storm (Q☒dm). During bypass conditions, the maximum water surface elevation and flow rate in the BMP will not be exceeded. Additionally, the hydraulic evaluation confirmed that the UFS does not impair the hydraulic capacity of the upstream drainage system during the 25-year design storm.

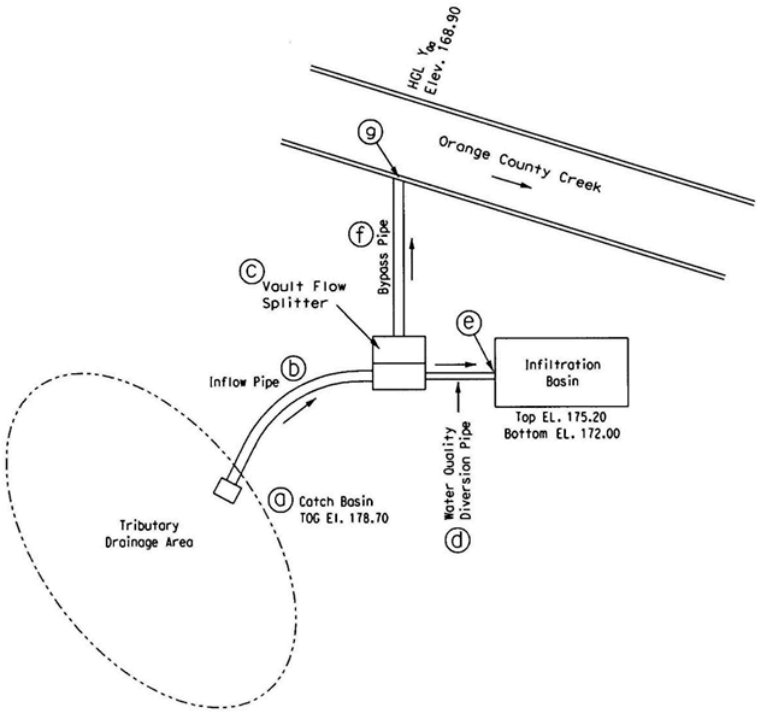

Figure 11: Plan of Project Site

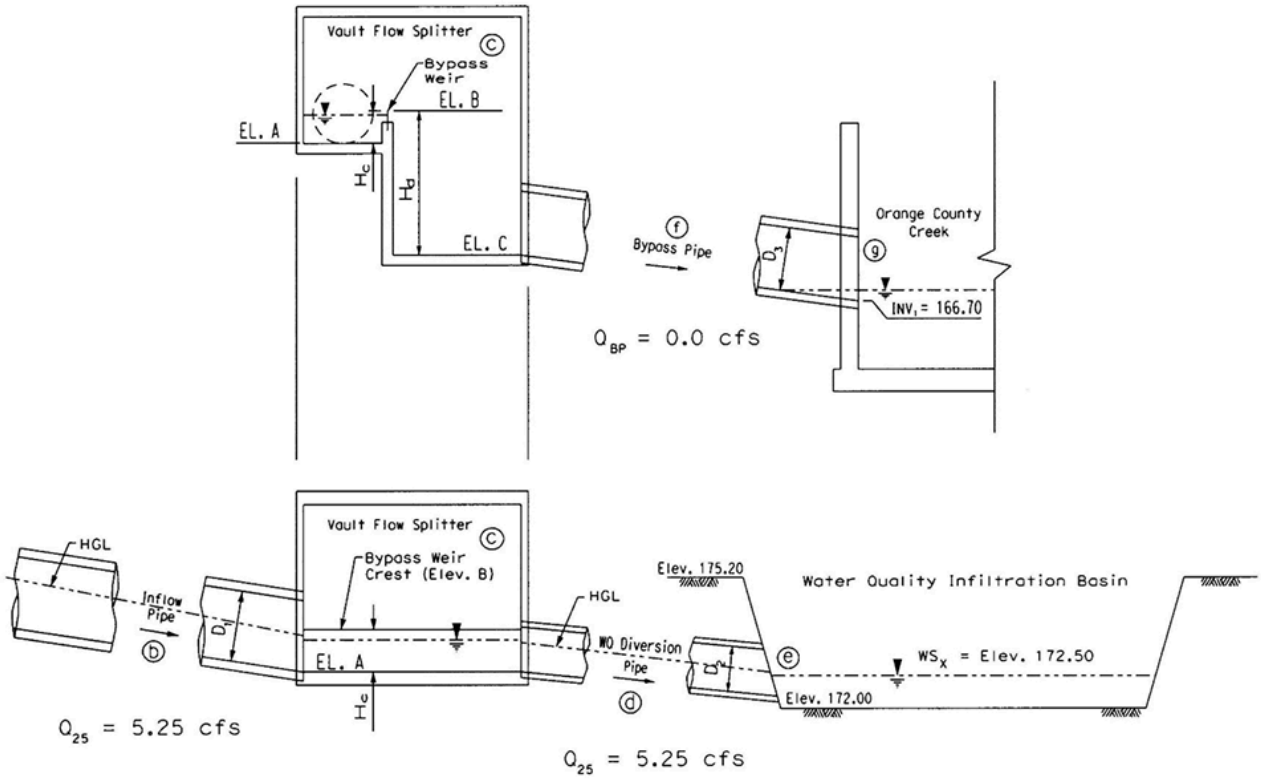

Figure 12: System Profile Showing Flow at Q25 Before Bypass

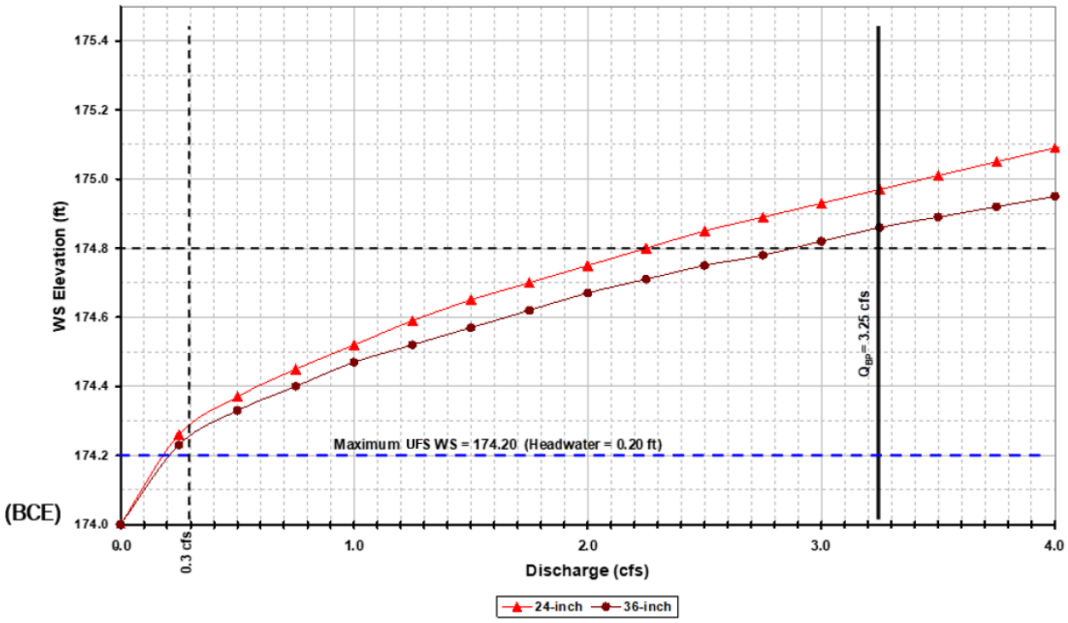

Figure 13: UFC Type 4- rating Curves

Sedimentation Tank

A research conducted by (Droste & Gehr 2018) to study the gravity-induced settling of particles with a density greater than the surrounding liquid is known as sedimentation.Basic settling tanks are commonly utilised for initial processing of water with high suspended solid content and for holding wastewater before treatment. These applications include:

- extracting grit from household sewage (often referred to as grit channels);
- holding raw sewage during stormy weather (typically called storm tanks, Figure 3.1) and
- equalising intermediate wastewater streams.

For lower concentrations of less dense solids, vertical and radial flow designs are employed. These are used for:

- eliminating large solids in primary wastewater treatment;
- removing flocs during water clarification;
- extracting lime softening precipitates;
- removing metal precipitates from industrial effluents and
- separating biomass in biological wastewater clarification.

Rectangular horizontal settling tanks are straightforward structures, typically measuring about 2m in depth with a length-to-width ratio ranging from 2 to 5 (Figure 14). These tanks feature an inlet at one end and an overflow weir at the opposite end for water discharge. As the water flows through, solid particles descend to the tank

bottom. A mechanical system, usually comprising a chain and flight scraper, is employed to gather the accumulated sludge, moving it towards one end for extraction (Figure 15).

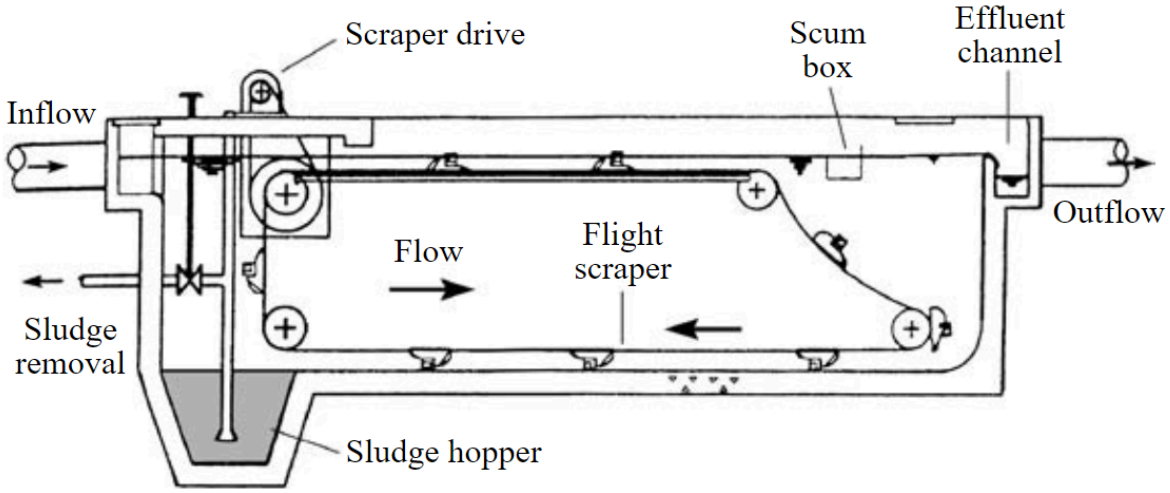

Figure 14: sedimentation tank (Droste & Gehr 2018)

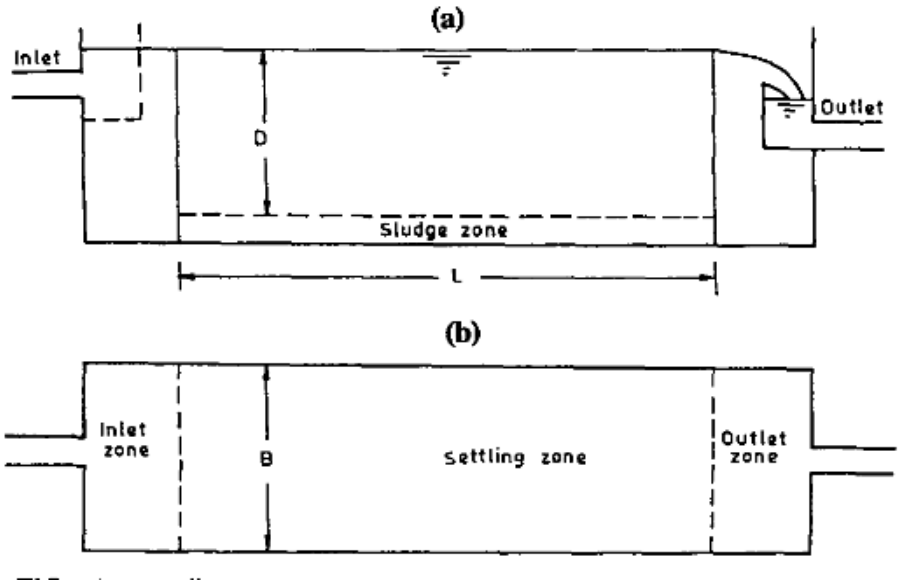

Figure 15: sedimentation tank model dimensions
(a) Longitudinal Section (b) Plan (Swamee & Tyagi 1996)

The design of primary settling tanks based on overflow rate and isoremoval plots, while widely used, has limitations in accurately predicting particle removal efficiencies across various operating conditions. A more

rational approach would involve considering the specific removal efficiencies of different particle sizes and the scour criterion of deposited particles. This method would take into account the settling velocities of various particle fractions and the critical shear stress required to resuspend settled particles, providing a more comprehensive understanding of the tank's performance.

By incorporating the removal efficiencies of individual particle size ranges and the scour criterion, engineers like (Swamee & Tyagi 1996) can optimise the design of primary settling tanks for specific influent characteristics and treatment goals. This approach would allow for more precise control over the removal of suspended solids and associated contaminants, potentially improving the overall efficiency of the wastewater treatment process. Additionally, considering the scour criterion would help prevent the resuspension of settled particles during high-flow events, ensuring more consistent performance and reducing the risk of carry-over to subsequent treatment stages.

(1) (Camp 1946) $V_0 = \frac{Q}{BL}$

$V_0 =$ *Overflow Rate*
$B \& L =$ *Width and length*

(2) (Rouse 1937) $\eta = 1 - P_0 + \int_0^{P_0} \frac{W}{V_0} dP$

$w =$ *Fall Velocity of the particle for the* proportion finer than P
$P_0 =$ *the fraction of the particles* $W \leq V$

(3) Stokes equation: $w = \frac{(s-1)gd^2}{18v}$

$s =$ *specific gravity of the particles*
$g =$ *gravitational acceleration*
$d =$ *particle size*
$v =$ *Kinematic viscosity of water*

(4) (Rouse 1937) $u_*/w \leq k$

$u_* =$ *shear velocity*
$0.5 \leq k \leq 0.8$

(5) (Cho & Sansalone 2013) $u_* = (\tau_0/\varrho)^{0.5}$

$\tau_0 =$ *average bed shear stress*
$\rho =$ *mass density of water*

(6a) (PK Swamee 1991) $P = \left[\left(d_*/d\right)^{m/m} + 1\right]^{-n}$

$m =$ *slope of the size distribution curve* j smaller diameters (Fig. 14)

(6b) $n = -1.4427 ln P_*$

$P = P_* \; d = d_*$

(7) $dP = m d_*^{-m} d^{m-1} dd$

(6c) $P = (d/d_*)^m$

$1 \leq m \leq \infty$ and $0 \leq n \leq 1$ with the increase in m and decrease in n the size of distribution tends to become more uniform. $d << d_*$

(8) $\eta = 1 - P_0 + \frac{m}{m+2}\frac{(s-1)gd_0^{m+2}}{18\upsilon V_0 d_*^m}$

From (2) (3), and (7) the removal efficiency was found

(9a) $d_0 = \left[\frac{18\upsilon Q}{(s-1)gBL}\right]^{0.5}$

$d_0 = particle\ size\ corresponding$ to the overflow rate $w = V_0$ and combining (1) and (3) find (9a)

(9b) $P_0 = \left[\frac{18\upsilon Q}{(s-1)gBLd_*^m}\right]^{0.5m}$

Combining (6c) and (9a)

(10) $\eta = 1 - \frac{2}{m+2}\left[\frac{18\upsilon Q}{(s-1)gBLd_*^2}\right]^{0.5m}$

When combining (6c) AND (9A) P0

(11) $d_0 = d_*\left[(0.5m + 1)(1 - \eta_D)\right]^{1/m}$

$\eta_D = design\ efficiency$ when combining (9a) and (10)

(12) Vq/BD

$D = depth\ of\ the\ tank$
$V > V_{sc}\ sludge\ velocity$ it will scour the particles $d_{sc} = particle\ size$

(13) $\tau_0 = \rho g D S_f$

Average tractive shear stress

(14) $S_f = \frac{fV^2}{8gD}$

$f = Darcy\ friction\ factor$
Combining (4), (13), (14), and settling $V = V_{sc}$ and $d = d_{sc}$ get (15)

(15) $V_{sc} = (\frac{8}{f})^{0.5}\frac{k(s-1)gd_{sc}^{\ 2}}{18\upsilon}$

$V_{sc} = sludge\ Viscosity$

(16) $f = \frac{0.316}{R^{0.25}}$

Friction for finished cement

(17) $R = 4Q/\eta\upsilon B$

$R = reynolds\ number$

(18) $f = 0.223(vB/Q)^{0.25}$ Eliminating R between (16) and (17)

(19) $V_{sc} = \frac{k(s-1)gd_{sc}^2}{3v}(\frac{Q}{vB})^{0.125}$ When combining (15) and (18)

(20) $V_{SC} = \frac{6kQ}{BL}(\frac{Q}{vB})^{0.125}$ $If\ V = V_{sc}$ and using (12) and (20) one gets

(21) $L = 6kD(Q/vB)^{0.125}$ $L = Length\ of\ settling\ tank$
K = 0.8

(22) $B = \frac{3.51Q}{d_0\sqrt{k(s-1)gD}}\left[\frac{v}{d_0\sqrt{k(s-1)gD}}\right]^{9/7}$

(23) $L = 5.13Kd\left[\frac{d_0\sqrt{k(s-1)gD}}{v}\right]^{2/7}$ d_0 = particle size

- Minimum depth lying between 1.5m and 2.5m for mechanically cleaned settling tanks. (Swamee & Tyagi 1996)

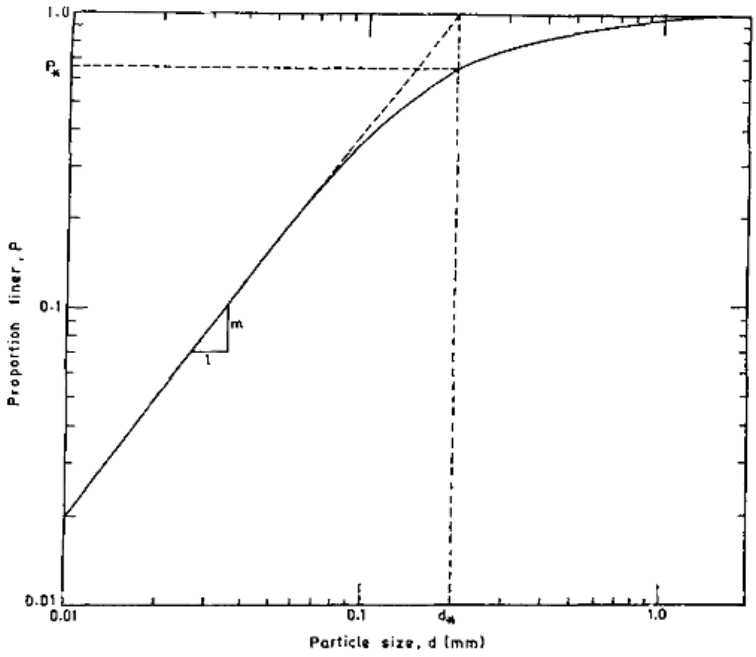

Figure 15: Particle size distribution curve (Swamee & Tyagi 1996)

The tank dimensions depend on the chosen dsc value. A small dsc leads to larger tank dimensions with only marginal increases in sediment yield. Conversely, a large dsc washes away most settled particles. As particles smaller than d0 progressively decrease due to removal in the influent, dsc can be assumed equal to d0. Using equations (9a) and (19) with this assumption, we can determine the tank dimensions.

IDALs: Intermittently decanted aerated lagoons wastewater

An alternate secondary process is IDALs. The IDAL anaerobic zone receives settled wastewater via pumping from the major distribution structure. To aid in the removal of phosphorus, discarded pickle liquor that is high in iron is added. Wastewater in IDALs passes through three steps in a single tank: settling, decanting, and aeration.

- Aeration: Through diffusers, air is injected into the IDAL. It reduces biological oxygen demand (BOD) by breaking down organic matter and water (nitrification) with the help of microorganisms in the tank.
- Getting settled: The water is motionless and there is no longer any air pumped into the tank. In the absence of oxygen, bacteria turn nitrates into nitrogen gas by using the carbon in organic matter as food. The atmosphere is exposed to the gas. Particles that are solid sink to the bottom.Before being treated for the manufacture of biosolids, some pass through a thickening tank. In order to supply microorganisms for entering wastewater, the remaining solids are sent back to the IDAL.
- Decanting: The clear wastewater settles and then runs into an equalisation basin from the top of the lagoon over weirs. The flow to the tertiary treatment process is managed by this basin.

Using traditional systems like aerated stabilisation ponds, aerated and non-aerated lagoons, and manmade and natural wetland systems is the most straightforward method for the anaerobic–aerobic treatment. These systems undergo anaerobic therapy at the bottom end and aerobic treatment at the top. The retention period ranges from a few days to 100 days, with an average organic loading of 0.01 kg BOD/m 3 days.(Wang et al. 2005)

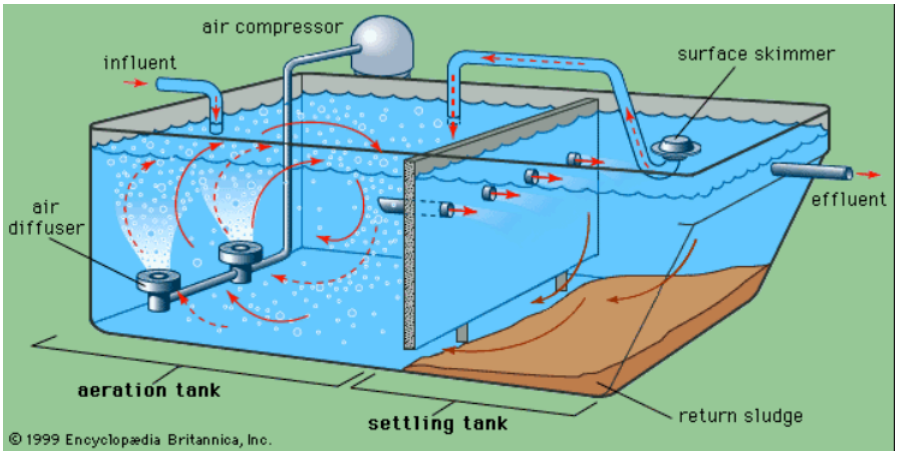

Figure 16: Diagram of IDAL's operation

For green olive debittering wastewater with COD ranging from 25,000 to 100,000 mg/L, (Aggelis et al. 2001) determined that neither anaerobic nor aerobic processes alone could effectively treat the waste. When dealing with such high-strength industrial wastewaters, singular anaerobic or aerobic treatment fails to produce effluents compliant with discharge limits. Utilising anaerobic-aerobic processes can reduce operating costs by a factor of eight compared to aerobic treatment alone, whilst achieving high organic matter removal efficiency, reduced aerobic sludge production, and eliminating the need for pH adjustment.

A study conducted by (Cakir & Stenstrom 2005) Cross-over points, which range from 300 to 700 mg/L influent wastewater ultimate BOD (BODu), are essential for aerobic treatment systems to operate efficiently. When treating influences at higher concentrations than the cross-over values, the benefits of anaerobic treatment exceed those of aerobic treatment, and anaerobic treatment often uses less energy with possible recovery of nutrients and bioenergy.However, aerobic systems remove more soluble biodegradable organic matter material than anaerobic systems do, and the biomass they produce is typically well flocculated, which lowers the concentration of suspended solids in the effluent. Consequently, an aerobic system's effluent quality is typically higher than an anaerobic system(Leslie Grady et al. 2009).
Anaerobic reactors are preferred for treating highly contaminated industrial wastewater due to their high COD levels, energy generation potential, and minimal excess sludge production.

However, practical applications face challenges such as slow microbial growth, poor settling rates, process instabilities, and the necessity for post-treatment of harmful anaerobic effluent containing NH_4^+ and HS^- found by (Heijnen et al. 1991). Despite the high efficiency of anaerobic processes, complete organic matter stabilisation is often unattainable due to the wastewater's high organic content. The resulting anaerobic effluent contains solubilised organic matter suitable for aerobic treatment, suggesting the viability of anaerobic-aerobic systems (Gray 2010) found the need for subsequent aerobic post-treatment to meet discharge standards.

(Vera et al. 1999) and (Cervantes et al. 2006) identified several benefits of the anaerobic-aerobic process:
• Significant resource recovery potential: Anaerobic pretreatment removes most organic pollutants, converting them into biogas, a useful fuel.
• High overall treatment efficiency: Aerobic post-treatment refines the anaerobic effluent, resulting in superior overall treatment efficiency and mitigating fluctuations in anaerobic effluent quality.
• Reduced sludge disposal: Digesting excess aerobic sludge in the anaerobic tank minimises total stabilised sludge production, lowering disposal costs and increasing gas yield.
• Low energy consumption: Anaerobic pretreatment acts as an influent equalisation tank, diminishing diurnal variations in oxygen demand and further reducing the required maximum aeration capacity.
• Effective volatile organic compound degradation: When present in the wastewater, volatile compounds are broken down during anaerobic treatment, preventing volatilisation in the aerobic stage.

(Leslie Grady et al. 2009) determined that the primary factor influencing microbial growth environments is the final recipient of electrons extracted during chemical oxidation for energy acquisition. These electron acceptors fall into three main categories: oxygen, inorganic substances, and organic compounds. An environment is deemed aerobic when dissolved oxygen is sufficiently available and not rate-limiting. This condition typically yields the

most efficient growth and a high ratio of biomass production to waste decomposition. Technically, any non-aerobic environment is anaerobic. However, in wastewater treatment, the term 'anaerobic' typically refers to conditions where organic compounds, carbon dioxide, and sulphate serve as the principal terminal electron acceptors, resulting in a highly negative electrode potential and less efficient growth. When nitrate and/or nitrite act as the primary electron acceptors in oxygen's absence, the environment is termed anoxic. The presence of these compounds leads to a higher electrode potential and more efficient growth compared to anaerobic conditions, albeit not as high or efficient as in aerobic environments.

The biochemical environment significantly impacts the microbial community's ecology. Aerobic conditions generally support diverse food chains, ranging from bacteria to rotifers. Anoxic environments are more restricted, while anaerobic conditions are the most limited, predominantly supporting bacterial life. The biochemical environment also influences treatment outcomes due to the varying metabolic pathways of microorganisms in these three environments. This distinction becomes crucial in industrial wastewater treatment, as certain transformations may occur aerobically but not anaerobically, and vice versa.

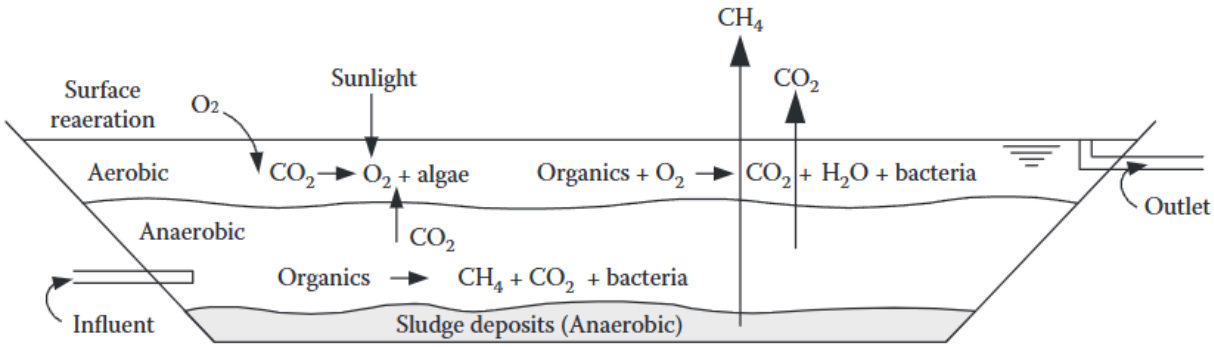

Figure 17: Chemical reaction of IDAL's(Leslie Grady et al. 2009).

In the past, lagoons have been constructed as expansive earthen reservoirs, reminiscent of typical "South Sea island lagoons" due to their size. Initially, these structures were unlined, but this approach proved problematic due to the risk of basin contents seeping into groundwater. As a result, current design standards mandate the use of an impermeable liner. The environmental conditions within lagoons can vary significantly, contingent upon the degree of mixing employed. Thoroughly mixed and aerated lagoons can maintain aerobic conditions throughout, whilst less mixing leads to solids settling, creating anoxic and anaerobic zones.

Completely mixed aerated lagoons (CMALs) are generally categorised as fully mixed reactors used primarily for soluble organic matter removal, although they can also facilitate the stabilisation of insoluble organic matter and nitrification. Facultative/aerated lagoons (F/ALs), as depicted in Figure 17, are mixed but not sufficiently to maintain all solids in suspension. Consequently, the upper regions tend to be aerobic, while the bottom contains anaerobic sediments. Anaerobic lagoons (ANLs) are not intentionally mixed; any mixing occurs solely due to gas evolution within them.

Lagoons represent one of the oldest biological wastewater treatment methods, with a history spanning over 3000 years(Rahman et al. 2019). They have been utilised as standalone treatment systems prior to surface water discharge, as well as for pretreatment and/or storage before conventional system or wetland treatment. A diverse range of industrial and municipal wastewaters has been processed using lagoon systems.

Theoretical consideration (Joe Middlebrooks et al. n.d.):

Ammonia-N removal in facultative wastewater stabilisation lagoons can occur through the following three processes:

1. Gaseous ammonia stripping to the atmosphere
2. Ammonia assimilation in algal biomass, and
3. Biological nitrification

Nitrification often does not account for a major amount of ammonia-N removal, as seen by the low quantities of nitrates and nitrites in lagoon effluents. Temperature, organic load, detention period, and wastewater properties all have an impact on ammonia-N assimilation in algal biomass, which is contingent upon the biological activity in the system. Temperature, pH level, and lagoon mixing conditions are the primary determinants of the rate of gaseous ammonia losses to the atmosphere. The equilibrium equation $NH_3 + H_2O \leftrightarrow NH_4^+ + OH^-$ is shifted toward gaseous ammonia by alkaline pH, whereas the mass transfer coefficient's magnitude is influenced by the mixing conditions. Both the mass transfer coefficient and the equilibrium constant are impacted by temperature.

(1) $$V\frac{dC}{dt} = Q(C_0 - C_e) - KA(NH_3)$$

$Q = flow\ rate,\ m^3/d$
$C_0 = influent\ concentration\ of\ (NH_4^+ + NH_3)$, mg/L as N
$C_e = effluent\ concentration\ of\ (NH_4^+ + NH_3)$, mg/L as N
$C = average\ lagoon\ contents\ concentration\ of\ (NI$, mg/L as N
$V = volume\ of\ the\ pond, m^3$
$k = mass\ transfer\ coefficient,\ m/d$
$A = surface\ area\ of\ the\ pond,\ m^3$ and
$t = time,\ days.$

(2) $$K_b = \frac{\left[NH_4^+\right]\left[OH^-\right]}{\left[NH_3\right]}$$

$K_b =$ *ammonia dissociation constant*

(3) $$\left[H^+\right] = \frac{K_w}{\left[OH^-\right]}$$

(4) $$C = NH_4^+ + NH_3$$

(5) $$NH_3 = \frac{C}{1+10^{pK_w - pK_b - pH}}$$

$pK_w = -\ logK_w$

$pK_b = -\ logK_b$

Assuming steady state conditions where $C_e = C$ find equation (6)

(6) $$\frac{C_e}{C_0} = \frac{1}{1+\frac{A}{Q}k\left[\frac{1}{1+10^{pK_W - pK_b - pH}}\right]}$$

$K = removal\ rate\ coefficient\ (1/t),\ and$
$f(pH) = function\ of\ pH$

(7) $$\infty e^{1.57(pH-8.5)}$$

Ammonia loss rate constant (Stratton 1969)

(8) $$\infty e^{0.13(T-20)}$$

(9) $$\frac{C_e}{C_0} = \frac{1}{1+\frac{A}{Q}K \bullet f(pH)}$$

$K = removal\ rate\ coefficient\ (1/t),\ and$
$f(pH) = function\ of\ pH$

(10) $$\infty_m = 10^{0.0413T-0.944}$$

$\infty_m = maximum\ specific\ growth\ rate, d^{-1}$
$K_N = half\ -\ saturation\ constant\ for\ ammonium\ n$
, mg/L
$T =$ *water temperature* ℃

(11) $$K_N = 10^{0.015T-1.158}$$

(12) $$\infty = \infty_m \frac{N}{K_N + Nk_{O_2} + O_2}[1 - 0.83(7.2 - pH)$$

$\infty = growth\ rate$
$N =$ *Concentration of dissolved oxygen*,mg/L
$O_2 = concentration\ of\ dissolved\ oxygen$,mg/L
$K_{O_2} = halfstauration\ constant\ for\ DO$,mg/L

(13) $$\frac{X_{N1}}{X_{N2}} = \frac{Q_R}{Q+Q_R}$$

Estimated ratio of Nitrifier
$Q = average\ flow\ rate\ through\ the\ basin, m^3/d$
$Q_R = recycle\ flow\ rate,\ m^3/d$
$X_{N1}/X_{N2} = ratio\ of\ nitrifier\ biomass$
Calculate the proportion of aerobic solids retention time. All nitrification was thought to

take place in Cell 2. It is necessary to create a suggested operating schedule that includes four one-hour settling and four one-hour discharging periods across the 24-hour cycle. For nitrifiers, the aerobic portion of the solids retention period will be 16/48, or 0.33.

(14) $$\theta_s = \frac{F_s}{f_{O_2}\left[1+\frac{X_{N1}}{X_{N2}}\right]\infty}$$

$\theta_s = solids\ retention\ time,\ d$
$F_s = safety\ factor$
$f_{O_2} = fraction\ of\ solids\ retention\ time\ that\ aerobic\ to\ the\ nitrifiers$
$X_{N1}/X_{N2} = ratio\ of\ nitrifier\ biomass$ concentration in cell 1 to that in cell 2

(15) $$X_{H2} = \frac{Y_H(S_0+X_{so})+F_1}{V_1/Q}\left[\frac{Q_s(Q+Q_R-V_1}{Q_R+(V_2/V_1)(Q+Q_R)}\right]$$

X_{H_2} = heterotrophic biomass concentration in cell 2, mg/L
$Y_H = heterotrophic\ growth\ yield$,mg biomass/mg$CBOD_5$
$S_0 = soluble\ CBOD_5\ of\ unwanted\ waste\ water,\ mg/$
$X_{SO} = particulate\ CBOD_5 of\ untreated\ wastewater,$
$F_1 = solids\ decay\ factor$[$Table\ Rich$(1999)]

(16) $$X_{H1} = \frac{Q_R X_{H2}+QY_H(S_0+X_{so})F_1}{Q+Q_R}$$

$X_{H1} = heterotrophic\ biomass\ in\ cell\ 1,\ mg/L$

(17) $$X_{i1} = QX_{io}\frac{V_2+Q_R\theta_S}{Q_R V_1+(Q+Q_R)V_2}$$

$X_{io}, X_{il}, X_{i2} = inert\ suspended\ solids\ concentrations$ (both organic and inorganic) in the influent wastewater, cell1 and cell2, respectively, mg/L

(18) $$X_{i2} = \frac{\theta QX_{io}-V_1X_{iL}}{V_2}$$

(19) $$X_{T1} = X_{H1} + X_{i1}$$

$X_{T1}, X_{T2} = total\ MLS\ in\ Cells\ 1\ and\ 2,\ respectively$

(20) $$X_{T2} = X_{H2} + X_{i2}$$

(21) $$P = 0.004X + 5$$

$(for\ X \leq 2000\ mg/L),\ P = power\ level,\ W/m^3$

(22) $$P = 8.125LnX - 48.75$$

$(for\ X \leq 2000\ mg/L)$,
$X = total\ suspended\ solids\ concentration,\ mg/L$

(23) $Q_a = 2.257 \times 10^{-3} + 0.244 \times 10^{-6}X -$

$Q_a = air\ flow\ rate\ at\ standard\ conditions,\ m^3 air/m$
$X = total\ suspended\ solids\ concentration,\ mg/L$

(24) $k_{d_{20}} = 0.480_s^{-0.415}$

$k_{d20} = specific\ decay\ rate\ at\ 20℃,\ d^{-1}$

(25) $k_d = k_{d_{20}}(1.05)^{T-20}$

$K_d = specific\ decay\ rate\ at\ T\ ℃,\ d^{-1}$

(26) $R_{O_2}1 = 4.16 \times 10^{-5}Q[1.47(S_0 + X_{s0}) -$

(27) $R_{O_2}2 = 4.16 \times 10^{-5}Q[4.57(N_0 + N_2) +$

(28) $P_{O_2} = 10^{3\frac{R_{O_2}}{NV}}$

$P_{O_2} = power\ intensity,\ W/m^3$

(29) $N_e = N_0 e^{-K_T[t+60.6(pH-6.6)]}$
$pH = 7.3e^{0.0005ALK}$

(Reid & Streebin 1979)

$N_e = effluent\ total\ nitrogen,\ mg/L$
$N_0 = influent\ total\ nitrogen,\ mg/L$
$K_T = temperature\ depending\ on\ rate\ constant$
$K_T = K_{20}(\theta)^{(T-20)}$
$K_{20} = rate\ constant\ at\ 20℃ = 0.0064$
$\theta = 1.039$
$t = detention\ time\ in\ system,\ d$
$pH = pH\ of\ near\ surface\ bulk\ liquid$

(30) $N_e = \frac{N_0}{1+t(0.000576T-0.00028)e^{(1.080-0.042T)(pH-6.6)}}$

(Middlebrooks & Pano 1983)

$N_e = effluent\ total\ nitrogen,\ mg/L$
$N_0 = influent\ total\ nitrogen,\ mg/L$
$T = temperature\ of\ pond\ water,\ degrees\ C$
$pH = pH\ of\ near\ surface\ bulk\ liquid$

Stirred tank Bioreactors aerobic treatment

Rather than utilising a single stirred tank bioreactor, it is recommended to employ a series of smaller stirred tanks, maintaining the same total volume as the single bioreactor. This configuration, which consistently enhances the overall bioreactor performance, is implemented in the activated sludge process through a technique known as step aeration (Rao & Subrahmanyam 2004), (Metcalf et al. 1991). The aerobic tank is segmented into multiple compartments, each receiving a separate burst of compressed air. The untreated wastewater enters the first compartment, with partially treated water flowing sequentially through subsequent compartments, and the final

treated effluent being discharged from the last compartment. Whilst this approach yields improved BOD reduction, it also incurs higher operational costs. As each compartment is relatively small and independently aerated, its performance may approach ideal behaviour (100% back-mixing). In contrast, a single large aerobic tank may contain dead zones and bypass streams, which disrupt back-mixing and negatively impact bioreactor performance.

To further enhance the bioreactor (aerobic tank) performance, a series-parallel arrangement of stirred tanks can be employed after research conducted by (Narayanan 2011) as well as (Leslie Grady et al. 2009). In this configuration, the aerobic tank is again divided into multiple compartments, with each receiving a portion of the raw wastewater and separate aeration. This method incorporates both step feeding and step aeration. Each compartment, except the first, receives a fraction of the fresh feed alongside partially treated effluent from the preceding compartment. This arrangement is particularly suitable for large-capacity installations. Here too, each compartment can function equivalently to an ideal continuous stirred tank reactor (CSTR), facilitating thorough contact between the substrate and biocatalyst (microbial cells). The performance equation for each compartment then becomes:

(1) $$\tau = (V/Q_0) = (C_{S0} - C_{Se})/(-r_{se})$$

$\tau = space\ time,\ s$

$V = reactor\ Volume,\ m^3$

$Q_0 = flow\ rate\ of\ substrate\ (feed),\ m^3/s$

$C_{SO} = substrate\ concentration\ in\ product\ solution,\ gL^{-1}\ or\ M$

$C_{Se} = substrate\ concentration\ in\ feed\ solution,\ gL^{-1}\ or\ M$

$C_{SP} = substrate\ concentration\ at\ biofilm\ liquid\ interface,\ gL^{-1}\ or\ M$

$-r_{se} = Monod\ type\ kinetics$

There is internal decay (albeit slight) and the bioconversion destruction) proceeds according to Monod-type kinetics.

(2) $$(-r_{Se}) = [(\mu_m/Y_e)C_{Se}x_e/(K_s + C_{Se})] - (k_d x_e)$$

$\mu_m = maximum\ specific\ growth\ rate,\ s^{-1}$

$Y_e = true\ yield\ coefficient$

$x_e = biomass\ in\ product\ solution$

$K_s = kinetic\ constant,\ gL^{-1}\ or\ M$

$K_d = endogenous\ decay\ coefficient,\ s^{-1}$

Equation 1 becomes:

(3) $$\tau = (C_{SO} - C_{Se})(K_S + C_{se})/F(C_s, x)$$

(4) $$F(C_s, x) = (\mu_m/Y_e)(C_{Se}x_e) - (K_s + C_{Se})(K_d x_e)$$

(5) $$(-r_s) = (\mu_m/Y)(C_s x)/(K_C x + C_s)$$

$K_s = Contois\ kinetic\ constant$

(Zabot et al. 2011) for dairy wastes

$Y = overall\ yield\ coefficient\ \ mg\ mg^{-1}$

(6) $\mu = [(\mu_m C_s)/(K_S + C_S)][K_N/(K_N + C_N)]$(Nara

$K_N = Liquid\ phase\ oxygen\ coefficient,\ g\ L^{-1}$

al. 2005)

The exceptionally high reactivity of nascent oxygen serves as the primary safeguard in LPO utilisation. Precise addition of hydrogen peroxide is crucial, as even a slight excess could destroy microbial cells, which explains the slow commercial adoption of LPO technology. Despite this, the H2O2 requirement remains low (5–7 M). It is feasible and often recommended to combine Membrane Based Technology with activated sludge processes. After preliminary treatments such as lime addition, coagulation, screen filtration and clarification, the wastewater can be fed into a reverse osmosis (RO) unit, producing reusable water as permeate. The RO concentrate then undergoes biological treatment in aerobic tanks and denitrification bioreactors. (Smith 1970) has documented a successful case study demonstrating enhanced BOD, phosphorus and nitrogen removal through the integration of RO with aerobic processes. (Narayanan 1993) has provided an economic analysis of this approach. The primary factors affecting the overall economy of RO systems are the operating pressure of the RO unit and the lifespan of the polymeric membrane, with membrane clogging and fouling presenting additional challenges. (Narayanan 1993) reported that by recovering two-thirds of the wastewater in the RO unit and subjecting the remaining third to biological treatment, the overall cost of treated water production could be reduced to three-quarters of conventional methods, including membrane replacement costs. Laboratory studies by (Thakura et al. 2015) have shown that employing a forward osmosis unit upstream and a nanofiltration unit downstream can achieve high chemical oxygen demand (COD) removal (exceeding 97%) from pharmaceutical wastewaters. However, the overall economic viability of this proposal requires analysis, considering the high operating costs of nanofilters and the substantial volume of wastewater typically handled in industrial settings.

Stirred tank bioreactors for anaerobic waste treatment

Similar to aerobic waste treatment study conducted by (Narayanan 2012), stirred tank bioreactors remain among the most popular choices for anaerobic processing of industrial, domestic and municipal waste, primarily due to their large capacity and straightforward installation. Anaerobic biological waste treatment, particularly when utilising a diverse culture of acidogenic, acetogenic and methanogenic microorganisms, offers the added benefit of converting organic matter into valuable products like biogas, a mixture predominantly composed of methane and carbon dioxide. The resulting anaerobic digested sludge can be utilised directly as a low-grade nitrogenous biofertiliser or employed in the production of phosphatic biofertiliser (known as Phosphate Rich Organic Manure) through biochemical means through (Sekhar n.d.) research.

However, the anaerobic digestion process is comparatively slower. Furthermore, methanogenic microbes, being obligate in nature, are highly sensitive to the medium's operating temperature and pH, with optimal conditions being pH= 7.0 and T=330–35°C. Anaerobic digestion can also be conducted at higher temperatures (55–65°C) using

thermophilic microbes, which accelerates pathogen destruction but incurs additional costs for heating pipe installation and external heat supply. The expense of extra energy input often negates the advantages of faster pathogen elimination and increased methane production. Moreover, thermophilic microbes generally grow more slowly than mesophilic ones. Unless waste heat is accessible, such as in Combined Heat and Power systems, thermophilic waste treatment is unlikely to be an attractive or beneficial option. Nevertheless, a thermophilic pretreatment may be applied to the feed slurry if pathogen destruction is a significant concern (Narayanan 2011).

$(-r_s) = (\mu/Y)x$

(Graef & Andrews 1974)

Kinetic

$\mu = (\mu_m C_s)/[K_s + C_s + C_s^2/K_{Si}]$

$K_{Si} = substrate\ inhibition\ coefficient,\ g\ L^{-1}$

$C_A = concentration\ of\ acetic\ acid\ in\ solution$

$\tau = (1/\mu)$

$\mu = (\mu_m C_A)/[K_s + C_A + C_A^2/k_{Si}]$

$K_a = ionisation\ constant\ of\ acetic\ acid$

$K_s = kinetic\ constant,\ gL^{-1}$

$C_A = concentration\ of\ unionised\ acetic\ in\ solutions,\ g/L$

$C_A = (K_1 C_{gL} C_{Se})/[K_a(C_{N0} - C_{Se})$

$K_1 = equilibrium\ constant\ of\ CO_2\ dissolved$

$C_{Se} = total\ concentration\ of\ acetic\ in\ solutions$

$C_{gL} = concentration\ of\ carbon\ dioxide\ in\ solutions$

$C_{N0} = concentration\ of\ ammonia\ in\ solution$

$\tau = (C_{gl}/R_c)$

$\tau = C_{gL}/[Y_C(\mu x_e) - (k_L a)(C_{gl} - C^*_{gL})\ ]$

$Y_c = yield\ coefficient\ for\ the\ production\ of\ CO_2,\ mol\ mol^{-1}$

$K_L = liquid\ phase\ mass\ transfer\ coefficient,\ ms^{-1}$

$a = specific\ interfacial\ area\ of\ mass\ transfer\ m^2 m^{-3}$

$\tau = C_{gL}/[Y_C(x_e/\tau) - (k_L a)(C_{gL} - He\ p_C)$

$He = henry's\ law\ constant,\ mol\ L^{-1} KPa^{-1}$

$P_c = partial\ pressure\ of\ CO_2 in\ the\ gas\ space\ kPa$

$Q(p_c/RT) = (k_1 a)(C_{gL} - Hep_C)V$

$Q = flow\ rate\ production\ of\ biogas\ m^3/s$

$C_g = molar\ concentration\ of\ CO_2\ in\ the\ gas\ space(C_g = pc/RT)$

$$Q\rho_g = Q(P/RT) = [(k_L a)(C_{gL} - Hep_c) + Y_m(\mu x_e)]V$$

$$\rho_g = molar\ density\ of\ biogas,\ mol\ m^{-3}$$

$$(Y_m x_e/\tau)[p_c/(P - p_c)] = (k_L a)(C_{gL} - He\, p_c$$

$$Y_m = yield\ coefficient\ for\ methane\ production,\ mol\ mol^{-1}$$

$$x_e = cell\ mass\ concentration\ in\ product\ solution\ g\ L^{-1}$$

Membrane packed bed biofilm technology (Bioreactor)

A bioreactor in wastewater treatment is a chamber that provides a controlled environment for microorganisms to break down organic contaminants in wastewater with packed bed biofilm reactors for wastewater treatment:

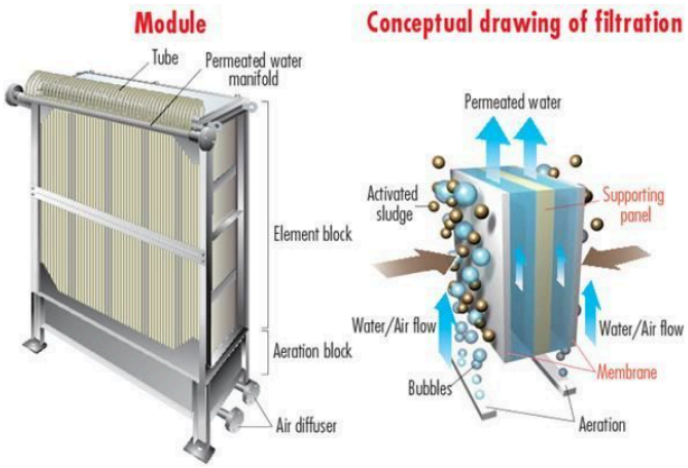

Figure 18: Membrane bioreactor diagram.

A specially designed chamber that supports the growth of bacteria and algae, also known as biomass. The bioreactor regulates factors like temperature, pH, oxygen concentration, and nutrient supply to create a controlled environment. Microorganisms break down organic contaminants into less toxic compounds. A membrane module separates the treated wastewater from the microorganisms. The membranes are permeable to water molecules, but trap other pollutants like bacteria, viruses, and suspended particles. The microorganisms attached to the filter can be self cleaned through the injection of oxygen when needed.

The membrane separation process and the activated sludge process are combined in a membrane bioreactor (MBR). Although subsequent clarification and tertiary processes like sand filtering are not required based on (Stephenson et al. 2000) research, the reactor functions similarly to a traditional activated sludge process.

Effluent and activated sludge are separated using low-pressure membrane filtration, either microfiltration (MF) or ultrafiltration (UF).In biofilm reactors, microorganisms develop in interconnected communities. These systems are characterised by multiple phases and handle diverse mixtures. With the exception of down-flow stationary fixed film (DSFF) bioreactors, which will be discussed subsequently, these reactors employ support materials such as silica granules, polymer beads, or activated carbon particles. Microbial cells form a biofilm that encases each of

these particles. Within these bioreactors, these particle-biofilm complexes constitute the discrete phase. The diameter of each aggregate (dPm):

(17) $d_{Pm} = (d_p + 2\delta)$

$d_{Pm} = diameter\ of\ aggregate$
$d_p = diameter\ of\ support\ particle$
$\delta = biofilm\ thickness$

(18) $\rho_{Sm} = f\rho_m + (1 - f)\rho_S$

$\rho_{Sm} = density\ of\ each\ aggregate$
$f = volume\ fraction\ of\ biofilm\ in\ aggregate$
$\rho_S, \rho_m = density\ of\ support\ particle\ and\ that$ of microbial cells respectively.

Microbial cells multiply and divide within the biofilm; nevertheless, when the biofilm's thickness exceeds a certain threshold, $0.3 < \delta < 0.5$

(19) $f = 1 - (d_P/d_{Pm})^3$

(20) $(-r_s) = \eta(-r_s)(int)$ $0.6 < \eta < 0.9$

(21) $\eta = a - tanh(\phi)[bcoth(n_d) - 1]/\phi$
(Leslie Grady et al. 2009)

(22) $\eta_d = (\sqrt{2}/\phi)((1 + \beta)/\beta\sqrt{\beta - ln(1 + \beta)}$

$\beta = (C_{SP}/K_s)$
$\phi = Thiele - type\ modulus$

(23) $\phi = L^* \sqrt{\mu_m(app)/(D_e K_s)}$

$L^* = characteristic\ dimension\ of\ particle$ biofilm aggregates

(24) $L^* = (d_{Pm}^3 - d_{Pm}^2)/(6d_{Pm}^2)$
$\mu_m(app) = (\mu_m/Y)x_f f(1 - \epsilon_{Pg})$

$a = 1, b = \eta_d, if\ \eta_d \leq 1$
$a = \eta_d, b = 1, if\ \eta_d \geq 1$
$\epsilon_{pg} = fractional\ gas\ holdup\ in\ fluidised\ bed$
$\epsilon_{pg} = fractional\ liquid\ holdup\ in\ fluidised\ bed$

(25) $\epsilon_P = (\epsilon_{PL} + \epsilon_{Pg})$

(26) $(1/\eta)^2 = (1/\eta_d)^2 + exp[\phi_b - (1/\eta_d)^2]$

(27) $\phi_b = 6\phi^2/\{5(1 + \beta)^2$

The membranes need to be cleaned periodically to maintain filtration performance. This is usually done weekly with chemical maintenance cleaning, and once or twice a year with recovery cleaning. The continuous filtration process eliminates a large portion of contaminants, ensuring that the treated water meets quality criteria.

Table 8: comparison of bioreactors.

Bioreactors	Merits	Limitation
Stirred tank	Easy to build and use. makes use of suspended microbial growth. Both anaerobic and aerobic processes can use it.	Low capacity only
Trickle bed biofuel reactor	use of microorganisms' associated growth. The downflow mode of operation results in low operational costs. The rate of bioconversion is accelerated by a high concentration of cell mass in the biofilm.	mostly for the aerobic elimination of BOD. reduced capacity as a result of the constant low input flow rate.
Moving bed biofilm reactor (slurry reactor)	a heterogeneous stirred tank variant. A high concentration of cells in the biofilm accelerates the pace of bioconversion.	less capable than column reactors in terms of capacity. The high rate of agitation could disturb the biofilm.
Fluidized bed biofilm reactor	Offers a high degree of bioconversion and operates at high volumes. The pressure drop over the bed doesn't rise when the feed flow rate increases once it has fully fluidized. Because of bed expansion, the degree of bioconversion rises as the feed flow rate increases.	Particle-biofilm aggregate entrainment loss may occur. Compared to trickling beds (packed beds), operating costs are higher.
Semi Fluidised bed biofilm reactor	Greater capacity and a lower reactor volume need for a higher degree of bioconversion (compared to fluidized beds). Even when the reactor volume remains constant, the degree of bioconversion rises as the feed flow rate increases.	more expensive to run than fluidized beds. It is impossible to operate in a continuous, circulating mode.
Inverse fluidised biofilm reactor	The downflow mode of operation results in low operational costs. Particles of a larger size could be employed. a respectably high level of bioconversion.	less capacity than a bed that is fluidized or semi-fluidized. greater need for reactor volume
DSFF bioreactor	Easy to build and use. No support particles are needed. The downflow mode of operation results in low operational costs. To improve capacity, more tubes or columns could be employed.	currently limited to anaerobic functioning. High capacity demands a large reactor volume.

UASB reactor	Easy to create. No particles of support were used. offers a significantly high degree of bioconversion at noticeably high capacities, even when the feedstock is strong.	limited to anaerobic procedures that use intricate microbial culture. excessively long starting time.

Mixing chamber flow analysis

Treatment methods and their impact on waste water (Anaerobic)

A study was conducted by (Abdelrahman et al. 2023) for wastewater treatment facilities to become more energy-efficient or even energy-neutral, biogas production from anaerobic sludge digestion is essential. A-stage treatment or chemically enhanced primary treatment (CEPT) in place of primary clarifiers are two examples of dedicated configurations that have been developed to maximise the diversion of soluble and suspended organic matter to sludge streams for energy production through anaerobic digestion.Because of the aeration energy demand, the A-stage design had the most energy consumption of the three, while CEPT had the highest operating expenses because of the use of chemicals. The utilisation of CEPT yielded the biggest energy surplus due to the highest percentage of recovered organic matter.

The preservation of ecosystems and public health depend on wastewater treatment. The primary purpose of wastewater treatment facilities (WWTPs) is to meet the necessary effluent criteria for nutrients and organics, which are expressed as chemical oxygen demand (COD) or biological oxygen demand (BOD). In addition, energy efficiency is becoming a bigger concern. In an effort to recover the energy and other resources contained in wastewater, WWTPs have even changed their name to water resource recovery facilities throughout the past ten years (Coats & Wilson 2017). Chemical energy (1.5 -- 1.9 kWh/m3 of wastewater) found in municipal wastewater is bound up in organic molecules′ chemical bonds (Scherson & Criddle 2014). Moreover, wastewater itself (4.6–7.0 kWh/m3 of wastewater) might be regarded as a thermal energy source.
The preservation of ecosystems and public health depend on wastewater treatment. The primary purpose of wastewater treatment facilities (WWTPs) is to meet the necessary effluent criteria for nutrients and organics, which are expressed as chemical oxygen demand (COD) or biological oxygen demand (BOD). In addition, energy efficiency is becoming a bigger concern. In an effort to recover the energy and other resources contained in wastewater, WWTPs have even changed their name to water resource recovery facilities throughout the past ten years (Coats & Wilson 2017). Chemical energy (1.5–1.9 kWh/m3 of wastewater) found in municipal wastewater is bound up in organic molecules′ chemical bonds (Scherson and Criddle, 2014; Hao et al., 2019). Moreover, wastewater itself (4.6–7.0 kWh/m3 of wastewater) might be regarded as a thermal energy source. Any substrate, including sludge, can be digested using the biomethane potential (BMP) test. In this test, the sludge in bottles is combined with inoculum that was taken from a functional digester(Abdelrahman et al. 2023).

(1) $$B(t) = B_0 . exp\left\{- exp\left[\frac{R_m . exp(1)}{Bo}(\lambda - t) + 1\right]\right\}$$

$B(t)$= *simulated cumulative methane yield (mL* CH_4/g *VS)*
$B(0)$ = *simulated highest cumulative methane yield (mL*$CH_4/g, VS$*)*
R_m = *maximum methane production rate* $(mL\ CH4/g\ VS{\cdot}d)$
λ = *Lag phase, biogas production*
R_m = *Maximum catabolic methane production*

(2) $$COD_{min} = COD_{Inf} - COD_{eff} - COD_{sludge}$$

$COD = (g/d)$

(3) $$COD_{methane} = \frac{Q_{methane}}{0.35} . COD_{sludge} . \left(\frac{VS}{COD}\right) sludge$$

VS = influent sludge
0.35 theoretical methane production/g
VS/COD = sludge ratio

(4) $$E_N = E_G - E_R - E_P - E_A - E_M - E_H$$
$E_N = Net\ energy\ recovery\ (Wh/m^3)$

$E_G = recovery\ of\ methane\ in\ biogas$
$E_R = energy\ consumption\ arm\ rotation\ in\ clarifier$
$E_P = sludge\ pumping$
$E_A = aerration$
$E_M = chemical\ tank\ mixing$
$E_H = Digester\ heating$

(5) $$E_G = \frac{Q_m . CV_m . E . 1000}{Q_{inf}}$$

$Q_m = m^3/d$ Flow rate production
$CV_m = (kWh/m^3)$ Calorific energy
E = Heat and electric conversion efficiency
$Q_{inf} = (m^3/d)$ Influent wastewater flow theoretical (1000 from kWh to Wh)

(6) $$E_R = \frac{W . r . v . 24}{e . Q_{inf}}$$

$W = N/m$ Arm loading factor
$r = m$ radius of tank (m)
v = tip velocity (m/s)
24 for h/d
e = efficiency

(7) $$E_P = \frac{Q_s . H . \rho . g}{e . Q_{inf} . 3600}$$

$Q_s = m^3/d$ Sludge rate production
H = pressure head
ρ = sludge density kg/m^3
g =gravity m/s^2

$3600 = s/h$

(8) $$E_A = \frac{COD_{Min} \cdot DO_{sat} \cdot 1000}{A.E \cdot (DO_{Sat} - DO_{Dis}) \cdot Q_{inf}}$$

$E_A = (Wh/m^3)$aeration energy consumption
$COD_{Min} = (KgCOD/d)$
$DO_{Sat} = (kg/m^3)$ saturated concentration
$DO_{Dis} = (kg/m^3)$ dissolved oxygen
$A.E = (kgO_2/kWh)$

(9) $$E_M = \frac{G^2 \cdot \mu \cdot V \cdot 24}{Q_{inf}}$$

$E_A = (Wh/m^3)$ *mixing energy chemical*
$G = (s^{-1})$*gradient velocity*
$\mu = (N.s/m^2)$
$V = m^3$*tank volume*
24 = h/d

(10) $$E_H = \left[\frac{Q_s \cdot (T_{AB} - T_{inf}) \cdot \rho \cdot C \cdot (1-\phi)}{3600 \cdot Q_{inf}}\right] + \left[\frac{A.(T_{AD} - T_{sur}) \cdot U \cdot 24}{Q_{inf}}\right]$$

$T_{AD} = temperature\ of\ anaerobic\ digest$
$T_{inf} = temperature\ of\ influent\ sludge$
$C = (J/kg \cdot °C)$ *specific heating capacity*
$\phi = heat\ recovery\ efficiency$
$A = (m^2)$ *digester surface area*
$T_{sur} = (°C)$*surrounding temperature*
$U = (W/m\,2 \cdot °C)$ *heat coefficient transfer*
$3600 = s/h$
$24 = h/d$

(11) $$C_{En} = C_{Tss}.\ TSS + C_{COD}.\ COD + C_N.TN + C_p.Tp$$

$C = (kg/m^3)$ *concentration in the effluent primary unit*
TSS, COD, TN and TP ($/kg)

(12) $$C_F = C_p.(1 + i)^n$$

$C_f = future\ value\ of$ ($)
$C_p = present\ value$ ($)
$i = interest\ rate$
n = *number of years*

To examine the destiny of influential COD, TN, and TP in each scenario, mass balances were set up (Figure 2). Of all the metrics, primary clarification had the lowest removal efficiency, whereas CEPT had the highest COD and TP removal efficiency. With a moderate TP removal rate of 32.2%, the A-stage's removal efficiency of COD (64.4%) and TN (22.8%) was comparable to CEPT. According to (Rahman et al. 2019), the influent entering sludge might contain 19–27% TN and 30–36% TP, which the A-stage could capture. Less COD was diverted to sludge for anaerobic digestion by the A-stage because 13% of the COD was lost through oxidation due to bacterial growth, which created

CO 2. This value matched the oxidation values that(Ge et al. 2017) reported. wherein the COD loss from oxidation at various operational SRTs (0.5-3 days) was less than 25%. It is anticipated that the side stream will be impacted if an A-stage or CEPT is included in place of a primary clarifier. According to the COD mass balance, integrating A-stage and CEPT may recover more COD from the wastewater—37 and 67%, respectively—for later conversion into methane gas than primary clarity. Since the COD/TN ratio in the effluent was low (around 3), which is favourable for Anammox bacteria (usually 2-3), partial nitritation-Anammox technology with minimal aeration needs can be applied for the treatment of effluent of the A-stage and CEPT (Zhang et al., 2019).

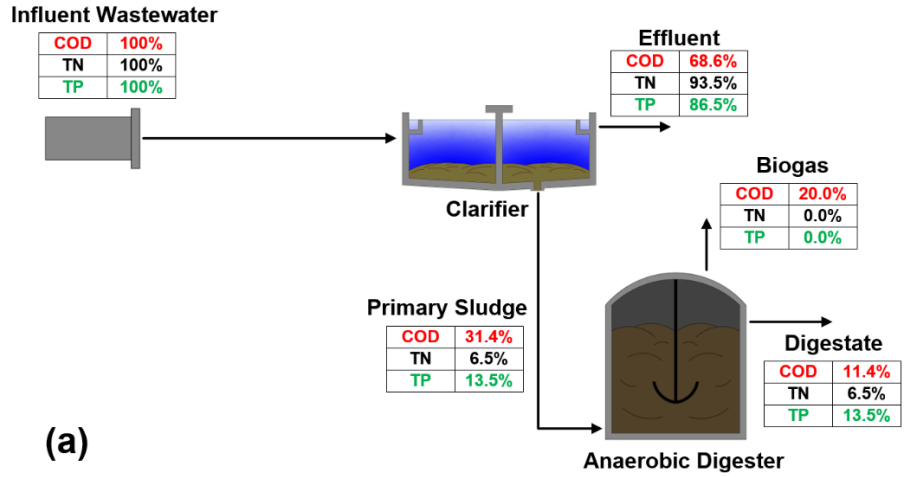

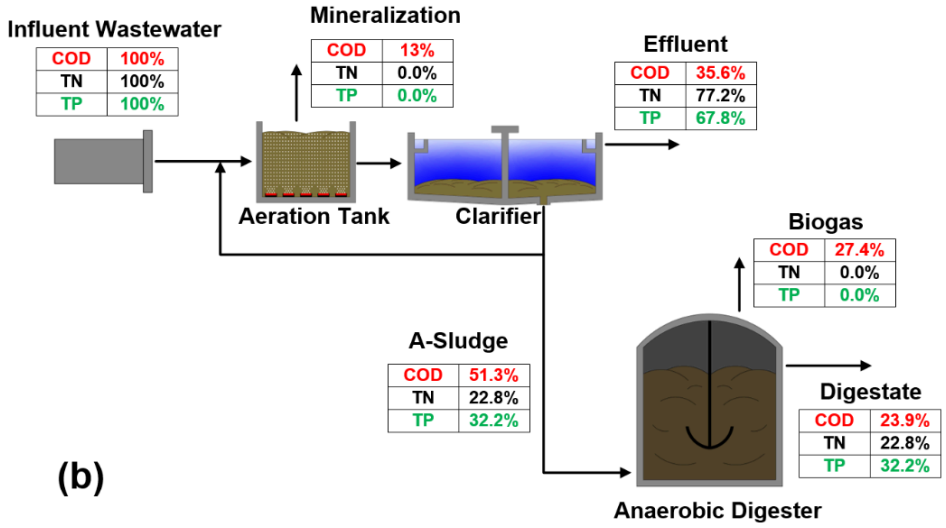

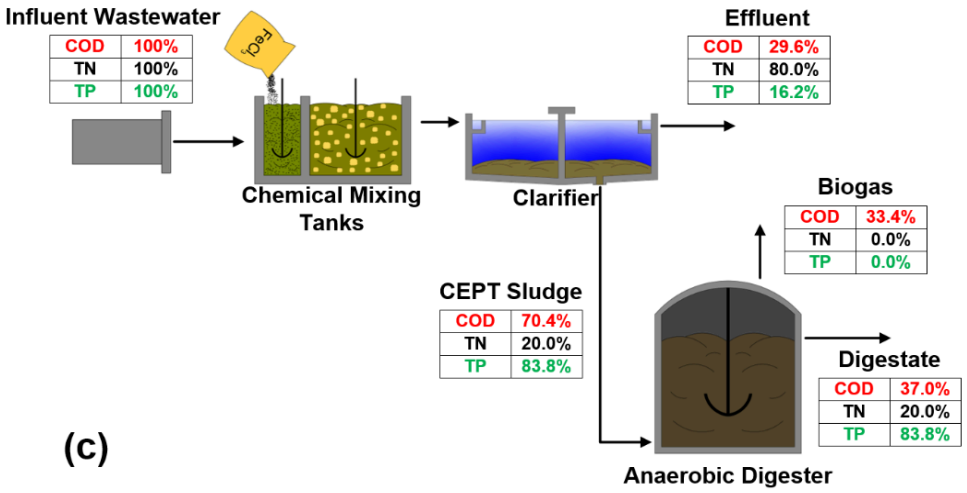

Figure 19 : COD, N and P mass balance: (a) primary clarification, (b) A-stage, (c) CEPT(Rahman et al. 2019).

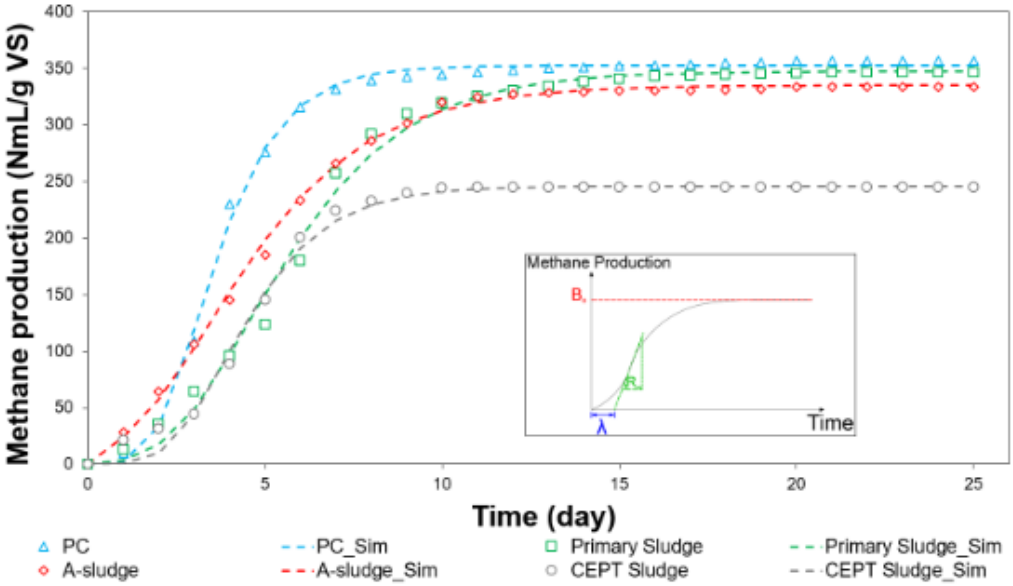

Figure 20: BMP results for each sludge after experimental stimulation(Rahman et al. 2019).

For every sludge, varying rates of methane generation and lag phases were noted (Figure 20). Consequently, rather than using a first-order rate model that was simplified, the modified Gompertz model was utilized to calculate the methane production (Kafle & Chen 2016). The updated Gompertz model (R2 > 0.95 for all curves) provided a good fit for the methane production curves (Figure 3). For main, A-, and CEPT sludge, the average B0 values were 347.3 ± 16.9, 335.0 ± 5.2, and 245.9 ± 5.5 mL CH 4/g VS, respectively. Out of all the sludges, the CEPT sludge had the greatest Rm (57.7 ± 0.6 mL CH 4/g VS·day) and λ (2.3 ± 0.1 day) (Figure 4). Primary sludge's kinetics were similar to those of CEPT sludge, with an average Rm and λ of 54.0 ± 2.0 mL CH4/g VS·day.and 2.2 ± 0.1 day, in that order. Table 1 shows that the digestion of A-sludge had the shortest lag phase (1.0 ± 0.0 day), which may be attributed to its comparatively high protein content. According to (Astals et al. 2014), proteins produced methane with a shorter lag

time than fats and carbs. Compared to other sludges, A-sludge had a somewhat lower Rm (49.0 ± 0.3 mL CH 4/g VS·day).

Characteristics	Primary Sludge	A-sludge	CEPT Sludge
Physicochemical Parameters			
TS (g/L)	53.73 ± 0.55	11.14 ± 0.21	27.46 ± 0.16
VS (g/L)	23.35 ± 0.09	5.73 ± 0.06	14.61 ± 0.08
VS/TS (%)	43.5 ± 0.4	51.4 ± 0.4	53.2 ± 0.2
COD (g/L)	36.27 ± 0.07	10.20 ± 0.02	21.27 ± 0.41
TN (%TS)	2.06 ± 0.05	5.54 ± 0.21	3.20 ± 0.05
NH_4-N (%TS)	0.54 ± 0.02	2.04 ± 0.05	0.75 ± 0.02
TP (%TS)	0.48 ± 0.01	0.69 ± 0.01	1.00 ± 0.06
pH	5.82 ± 0.02	7.31 ± 0.01	7.25 ± 0.01
Organic fractions			
VFA (mg/g VS)	42.6 ± 1.4	17.3 ± 1.1	9.2 ± 0.1
Proteins (mg/g VS)	208.2 ± 7.8	403.4 ± 28.5	261.9 ± 15.9
Lipids (mg/g VS)	234.2 ± 10.0	158.6 ± 12.0	123.2 ± 11.5
Soluble carbohydrates (mg/g VS)	9.0 ± 0.3	8.4 ± 0.0	11.7 ± 0.8
Cellulose (mg/g VS)	195.5 ± 31.6	98.8 ± 17.0	41.7 ± 11.1
Hemi-cellulose (mg/g VS)	194.5 ± 14.9	121.6 ± 18.8	130.3 ± 25.5
Lignin (mg/g VS)	87.1 ± 6.5	50.0 ± 7.7	180.9 ± 19.1

Table 8: Sludge characteristics(Rahman et al. 2019).

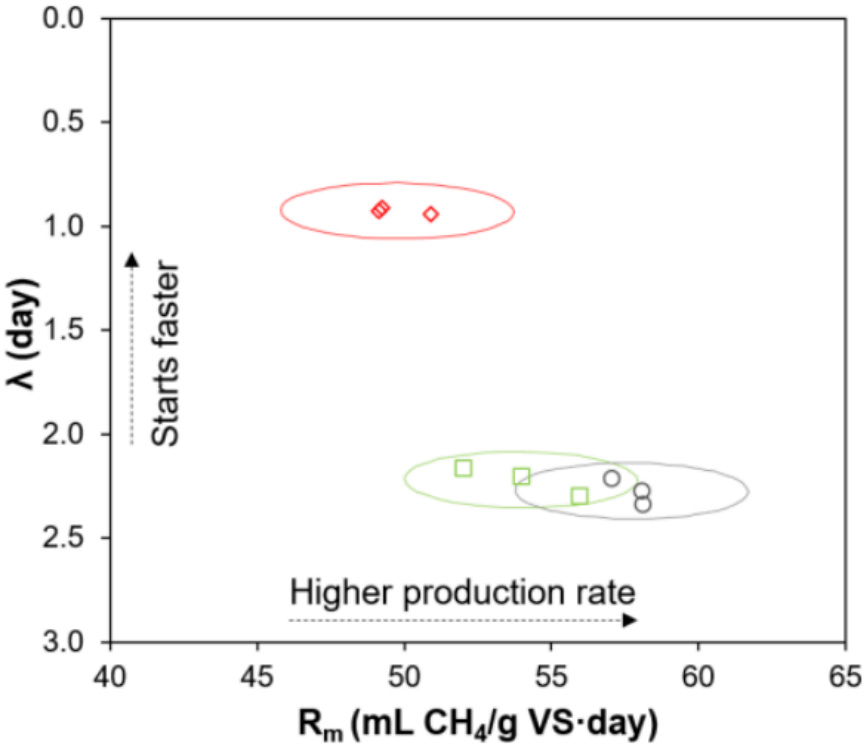

Figure 21: The relationship between the lag phase (λ) and the maximal methane production rate (Rm) for every sludge. Each sludge type's three identifiers denote triplicate samples. A 95% confidence level is represented by the circle.

Dual Media Filter

Access to clean water is crucial for human survival, ecosystem preservation, and societal well-being. The process of treating drinking water is intricate, involving various stages that are determined by regulations, contaminant elimination objectives, and associated expenses. In 1854, a breakthrough occurred when it was discovered that a cholera outbreak was transmitted through water. Areas with sand filters in place experienced less severe effects. British researcher John Snow (Belford 2013) identified that the primary cause of the epidemic was the contamination of a water pump by sewage. He utilised chlorine to sanitise the water, laying the groundwork for water disinfection techniques. This finding prompted governments to implement municipal water filtration systems, comprising sand filters and chlorination, marking the inception of public water regulation. Since that time, filtration has remained at the core of drinking water treatment, alongside disinfection, for more than a hundred years.

A study conducted by (Lund n.d.) in Scotland, water treatment primarily focuses on addressing pathogens and organic compounds, largely due to the region's landscape and prevalent livestock farming practices. This has led to a significant interest in enhancing treatment efficiency. Conventional filtration methods utilise granular media,

such as sand, in either rapid or slow filters, depending on the applied flow rate. During the latter half of the 20th century, dual media configurations were introduced, incorporating an anthracite layer on top and occasionally a third thick gravel layer. Although these methods remain widely employed globally and have demonstrated their reliability and effectiveness, recent legislative changes and a general drive towards greater efficiency have spurred research into alternative approaches. These new avenues of investigation encompass not only process modifications and the application of novel materials to improve treatment performance but also aim to reduce costs and, crucially, enhance energy efficiency.

Filtration Process

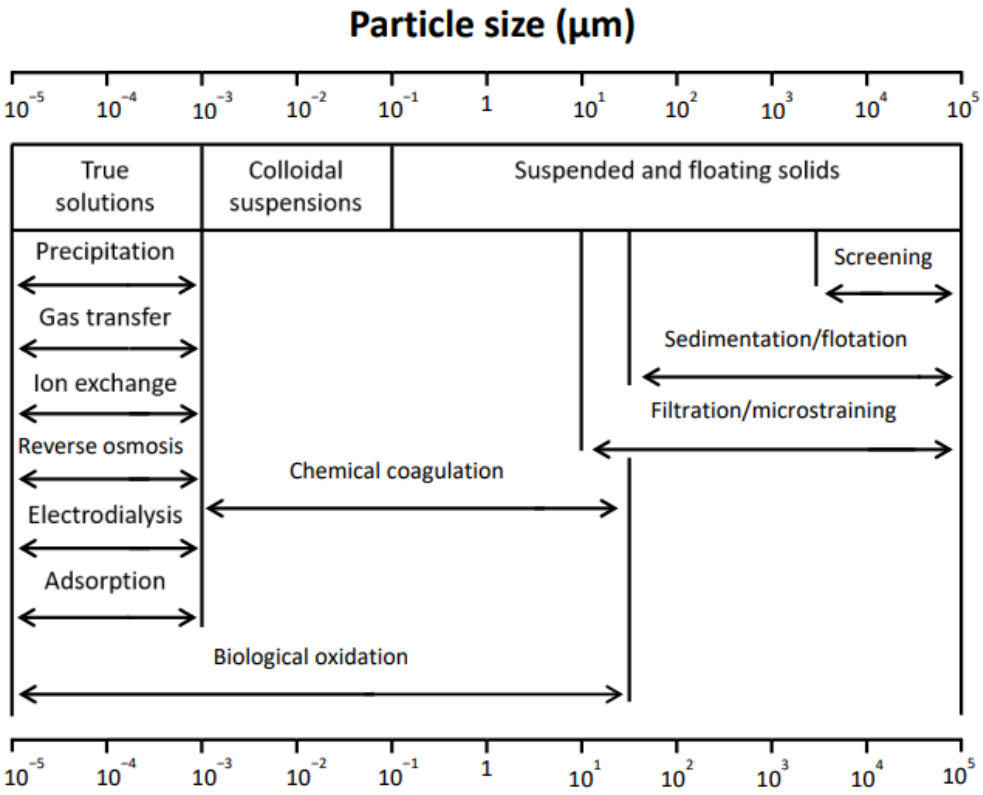

Figure 22: Treatment processes with respect to range of effectiveness (Tebbutt 1997).

The efficacy of filters is determined by several physical properties, including grain size, shape, porosity, and the relationship between bed depth and media grain size. For filter bed design, a research conducted by (Kawamura & McGivney 2007) proposes utilising the L/de ratio, where L denotes the filter bed depth (mm) and de represents the effective size of the filter medium. This ratio fluctuates between 1000 and 2000 for various filter configurations, with specific ranges for different media types. The authors also recommend increasing L/de ratios by 15% to achieve filtered water turbidity under 0.1 NTU, and suggest conducting pilot studies when selecting filter depths for media exceeding 1.5 mm in size.

Filtration processes can be categorised as either depth or cake filtration. Depth filtration involves particles being captured within the medium's pore network, while cake filtration results in a layer forming on the medium's surface through (Cheremisinoff 2019) research. Granular media filters predominantly function through depth filtration studied by (Gray 2010) . The filtration mechanism comprises two primary stages: transport, which moves particles towards the filter media, and attachment, which is contingent upon particle-surface interactions. These stages are not entirely discrete, as attachment mechanisms may cause particles to deviate towards the grain surface through a study conducted by(Charles R. O'Melia n.d.). Some researchers argue that transport mechanisms exert a greater influence than surface forces (Ison & Ives 1969) . Particle aggregation can also occur, forming clusters that are more readily transported and deposited. An additional stage, detachment, allows particles to re-enter the flow(Zamani & Maini 2009).

Research into deep bed filtration has conceptualised filter beds as assemblages of individual collectors, with efficiency calculated based on uniform spheres acting as collectors (Rajagopalan & Tien 1977). The removal at any given plane is a function of the number of collectors within that distance. This approach transforms the problem into one of particle transport and deposition onto individual grains, referred to as trajectory analysis or the microscopic model.

The analysis of particle trajectories is only applicable to a pristine filter; as particles accumulate, they alter the filter bed's characteristics and flow patterns. Deposited particles serve as additional collection points for subsequent particles (Amirtharajah 1988), necessitating their inclusion in efficiency calculations. Some researchers contend that these accumulated particles may be more effective collectors than the original filter grains (O'Melia & Ali 1979).

The filtration process comprises several phases (Figure 23). (Ison & Ives 1969) identify an initial clean filter stage, followed by a transitional phase. During this transition, filter performance initially improves (ripening), then stabilises during a working stage, before ultimately declining during breakthrough. The performance enhancement results from increased particle deposition, which eventually leads to higher velocities and reduced deposition. Breakthrough occurs when insufficient filter bed depth remains for particle removal, necessitating the termination of the filtration run. However, most researchers disregard the initial stage as atypical of average filtration runs, focusing instead on the three components of the transitional stage (Graef & Andrews 1974).

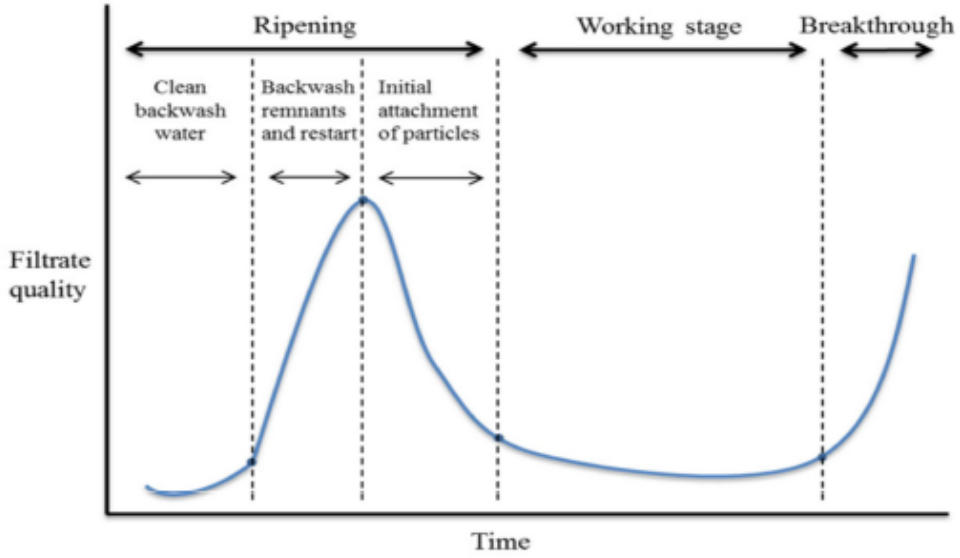

Figure 23: Cycle of filtration (American Water Works Association 2011).

Absorption Sorption process

The primary parameter in adsorption operations is the empty bed contact time (EBCT) studied by(Stuetz & Stephenson 2009) , which is calculated by dividing the volume of adsorbent by the flow rate. The EBCT for most water treatment applications is between 10 and 20 minutes. As long as the carbon at the bottom of the bed is not exhausted, the organic waste is normally removed at a rate greater than 99%.
Adsorption capabilities are high: typical commercial activated carbons may absorb up to 20% of their weight in organic compounds from water.

Figure 24: granular activated carbon tank.

Empty bed contact time: (Stuetz & Stephenson 2009)

$EBCT = V/Qh$

$V = volume\ of\ GAC\ (m^3)$

$Q = flow\ rate\ (m^3 h^{-1})$

Adsorption is mostly used to remove organic materials from water and, occasionally, wastewater. Duties include removing taste, odour, colour, THM precursors, pesticides (before or after ozonation), natural organic matter, dechlorination, de-ozonation, solvents, and COD from industrial wastewater.

Filtration operation setup

The configuration of filtration systems influences their effectiveness. Single sand medium filters often fall short in meeting treatment requirements, leading to the development of dual media filters. These employ a denser material at the bottom and a lighter one on top, with decreasing particle size. The most common arrangement features an anthracite layer above a sand layer, sometimes with an additional garnet layer (Ratnayaka 2009). While the filtrate quality is comparable to sand filters, dual media filters can operate 1.5–3 times longer at similar filtration rates. Efforts to increase filtration rates in dual configurations have been made, often involving coagulation aids. The size of coagulation-induced flocs is crucial; if too small, they may pass through the first layer and rapidly clog the sand layer, while overly large flocs could quickly obstruct the anthracite layer (Ratnayaka 2009). Anthracite's effective size is typically 1.5 mm, though this varies globally. The anthracite layer is usually 150–300 mm deep, with the sand layer at 450–600 mm (Twort et al. 2000), although (Belford 2013) suggests the reverse proportion.

(Zouboulis et al. 2007) conducted a comparative study of single medium sand and dual media sand/anthracite filters for conventional and direct filtration. In conventional filtration, the dual media setup operated for longer

cycles, yielding 10% more water production. Dual media cycles lasted 2–3 times longer than single medium cycles, with final head loss values less than half (Figure 25a). Both configurations achieved turbidity levels well below 0.2 NTU, with the dual media setup performing slightly worse (Figure 25b). Direct filtration proved more challenging to manage. With low coagulant doses, the single medium filter failed to meet the required turbidity level, showing values of 0.5–1 NTU. The dual media filter demonstrated greater efficacy, achieving turbidity values marginally higher than those in conventional operations (0.2–0.3 NTU) (Zouboulis et al. 2007).

An attempt was made to employ anthracite in coarser mono-medium filters with a deeper bed (1.8 m) in order to adopt greater filtration rates, but this approach was quickly given up by (Logsdon et al. 2006). The primary problems with anthracite are its high price and scarcity of global supplies; as a result, high-grade bituminous coal has occasionally taken its place (Ratnayaka 2009). In certain situations, other materials have been employed, such as GAC instead of sand or anthracite to eliminate smells. To boost the effectiveness of the GAC, it is more typical to add an adsorption step with a longer contact time after the filter (Logsdon et al. 2006).

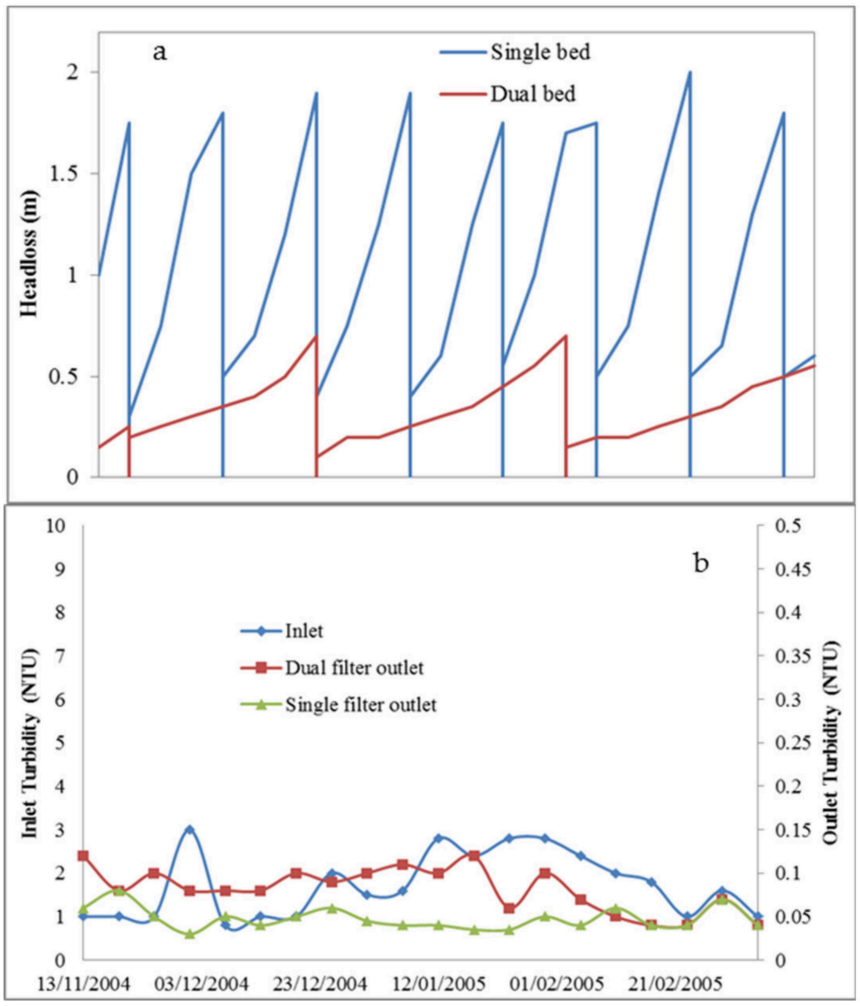

Figure 25: a- Head loss development, b- turbidity due to conventional treatment(Zouboulis et al. 2007).

A significant issue associated with backwashing is the elevated turbidity observed when the filter resumes operation. This period, known as ripening (Figure 23), occurs due to the loss of particles that aid filtration and the incomplete removal of flocs during the final stages of backwashing study by (Slavik et al. 2013). Three distinct phases have been identified: initially, the filtrate is influenced by residual backwash water in the filter underdrains, followed by contaminants remaining above and within the filter bed.
Lastly, the filter's efficiency is compromised by the absence of additional particle retention capacity (Slavik et al. 2013) . This problem has garnered increased attention as studies have shown that Giardia and Cryptosporidium cysts may be transmitted during this phase (Amirtharajah 1988). Various methods exist to mitigate this issue, including introducing coagulants to the backwash water or influent upon filter restart, implementing a terminal sub-fluidised rinse, allowing the filter to rest (delayed start), discarding the initial effluent (filter-to-waste), and adjusting filter rates (beginning with low rates and gradually increasing; termed slow start) (American Water Works Association 2011). It is considered typical for a filter to produce effluent with 0.5–1 NTU turbidity after restarting, which should then decrease to 0.2 or less within the first 30 minutes of operation and to 0.1 after an additional hour(Spellman 2008) . (Logsdon et al. 2006) suggests a target of 0.3 NTU post-backwashing, dropping below 0.1 NTU within 15 minutes of resuming service.

Chlorination

The finest and least expensive disinfectant operator for deactivating germs and ensuring their persistence to assure their growth in the water supply network. Waterborne illnesses like cholera, typhoid fever, and dysentery were significantly reduced in assuring human health due to chlorine disinfection (Calderon 2000). Disinfection of municipal water with chlorine has provided significant community health benefits by controlling contagious diseases; however, in raw water, the contact of natural organic matter (NOM) with chlorine produces chlorination disinfection by-products (DBPs), particularly trihalomethanes (THMs) and haloacetic acids (HAAs), which are of health concern (Bellar et al. 1974);(Rook 1972). DBPs' regular use in modest amounts may have a negative impact on human health, with a focus in the past on their cancer-causing nature. The generation of THMs in chlorinated water is determined by the raw water composition, operational characteristics, and residual chlorine in the water delivery network.

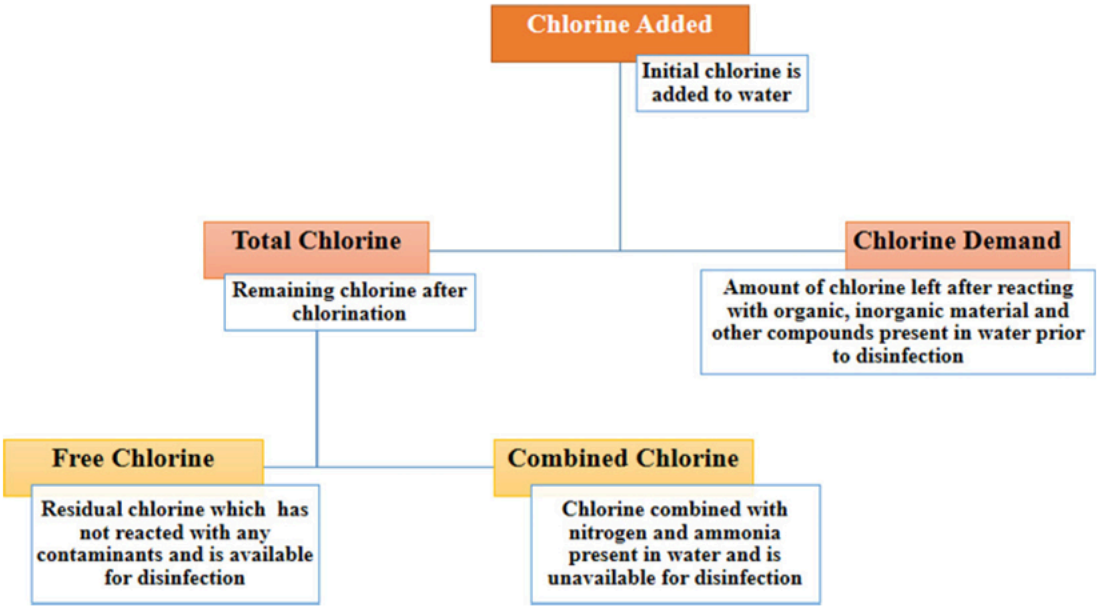

Figure 26: flowchart demonstrating chlorine addition (Ruyack 2019).

(Mazhar et al. 2020) demonstrated that when chlorine is added to water, a portion of the chlorine reacts with inorganic and natural elements and metals present and is not available for disinfection, which is known as the chlorine demand of water, and the remaining chlorine is known as total chlorine. Total chlorine is divided into mixed and free chlorine. When chlorine mixes with inorganic compounds such as nitrates and organic nitrogen-containing molecules such as urea, it functions as a weak disinfectant that is inaccessible for disinfection. The free chlorine is the residual chlorine that can be used to inactivate microorganisms; it is a measure of the water's potability. Thus, the sum of combined chlorine and free chlorine yields the total chlorine necessary. For example, when using completely clean water with no impurities, the chlorine demand is zero, and the combined chlorine demand is likewise zero because no inorganic or organic material is present in the water. In this method, the free chlorine concentration will be equal to the applied chlorine. Because of the existence of organic matter in surface water supplies, there will be a demand for chlorine, which will be met by inorganic chemicals such as nitrates. The free chlorine will be calculated as the sum of total and combined chlorine demand. (Figure 26) depicts a flowchart for the addition of chlorine.

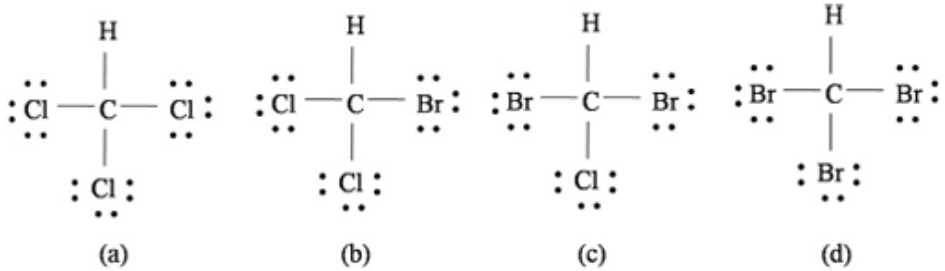

Figure 27: Chemical structures (a) chloroform (b) Bromodichloromethane (c) Dibromo-chloromethane (d) Bromoform.

The equation below applies to the production of DBPs:

$NOM + HOCL + Br \rightarrow DBPs\ (THMs\ and\ other\ halogenated\ products)$

THMs, primarily comprising chloroform, dibromochloromethane (DBCM), bromodichloromethane (BDCM), and bromoform, are formed during chlorination when NOM precursors such as humic and fulvic acid react with chlorine (Thokchom et al. 2020). These DBPs are present in chlorinated water, with chloroform typically being the most prevalent THM. When bromide is oxidised in the presence of precursors, brominated THMs are produced. Some THMs are considered potentially carcinogenic to humans. Although chloramination generates lower THM concentrations compared to chlorination, it also produces cyanogen chloride as an additional DBP (Duong et al. 2003). Ozone can oxidise bromide to form hypobromous acid, a brominated THM precursor, whilst chlorine dioxide does not create THMs when reacting with organic precursors.

THMs are chemical compounds derived from methane CH_4 where three of the four hydrogen atoms have been substituted by halogens. The main THMs formed in drinking water due to chlorination are dibromochloromethane $CHCLBr_2$, bromodichloromethane $CHCL_2Br$, and bromoform $CHBr_3$, with chloroform $CHCL_3$ being the most common. Their chemical structures are illustrated in the accompanying figure 27.

It is necessary to do extensive research to comprehend the chemistry of DBPs′ occurrence in each situation in order to identify the best controlling approach. However (Mazhar et al. 2020) research have determined that, lowering the DBP level prior to, during, and following water treatment comes with a cost.Therefore, as a way to reduce the health risk associated with these DBPs, the recommendations values must be closely enforced in order to lower the permissible exposures or concentrations. There have been attempts to limit DBPs only by more stringent regulations.

Dissolved air flotation

The decrease in pressure of an air-saturated water stream creates the bubbles in DAF. Pressure flotation is the most significant and frequently utilized of the three DAF types—vacuum flotation, microflotation, and pressure flotation—in the treatment of water and wastewater. Pressure flotation creates tiny air bubbles by dissolving air in water at high pressure and releasing it at atmospheric pressure via a needle valve or nozzle.

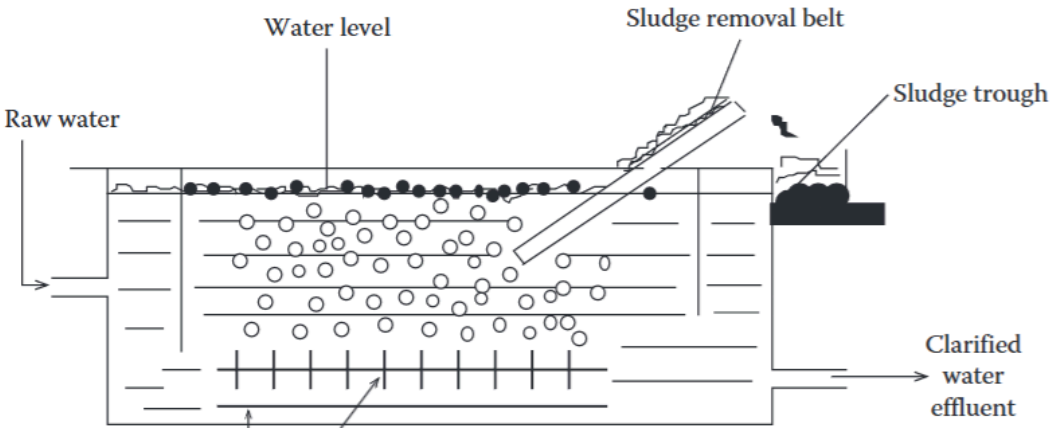

Figure 28: Kinetic foam floatation diagram through aid diffusion (Adlan 1998)

Bubbles that lower the density of the bubble–particle agglomerates cause the particles to float during the DAF process. Bubble-particle agglomerates will rise and float to the top as long as their density is lower than that of water (1.00 g/cm 3). Compared to large particles, which need more bubbles to reduce density, small particles require fewer bubbles. The flotation tank's surface should be reached by the bubble-particle agglomerates (Adlan 1998). The cleared water is used to sweep out the agglomerates that do not rise to the surface. Stokes' law can be used to estimate the bubble-particle's increasing velocity.
The three primary DAF theories demonstrate that before using the DAF system for water or wastewater treatment, certain parameters impacting the system should be taken into account. Therefore, when constructing and using the DAF system, all elements and system operation should be taken into consideration.

(1) Stokes law (Li & Lam 1964)	$D = 6\pi a\mu U$	$D = drag\ force\ (kN)$ $a = radius\ of\ bubble\ (m)$ $\mu = dynamic\ viscosity\ (kg/m/s)$ $U = terminal\ velocity\ (m/s)$
(2)(Packham & Richards 1972)	$\frac{4}{3}\pi a^3\sigma g = \frac{4}{3}\pi a^3\rho g + 6\pi a\mu U$ $U = \frac{2}{9}(\sigma - \rho)a^2\frac{g}{\mu}$	$a = radius\ of\ sphere\ (m)$ $\sigma = density\ of\ sphere\ (kg/m^3)$ $\rho = density\ of\ liquid\ (kg/m^3)$
(3)(Jameson 1984)	$6\pi\mu Ua = \frac{4}{3}\pi a^3(\varrho - \rho_g)g$	$\rho_g = density\ of\ gas,\ negligent$
(4)	$U = \frac{2\rho g a^2}{9\mu}$	

(5)(Harper 1972)

$$C_D = \frac{Force\ on\ bubble}{1/2U^2\pi a^2} = \frac{4/3\pi\rho g a^3}{1/2\rho U^2 a^2} = \frac{4gd}{3U^2}$$

$C_D = drag\ coefficient$

(6)

$$C_D = \frac{24}{Re}$$

$Re = Reynolds\ number\ < 0.5$

(7)(Fukushi et al. 1995)

$$U = \frac{pga^2}{3\mu}$$

$a << 2 \times 10^{-2} cm$

(8)

$$\frac{ga^3}{3v^2} << 1$$

$\nu = \mu/\rho$

(9)

$$R = 1 - e^{-(\frac{V_r}{Q/A_h})}$$

$R = ratio\ of\ total\ removal\ of\ solid\ concentration\ after\ flotation\ to\ the\ inflow = 1 - C_0/C_i$

$C_0 =$ *the effluent suspended solids*

$C_i = the\ influent\ suspended\ solids$

$V_r = the\ rising\ velocity\ of\ a\ single\ particle/ai\ Bubble\ (m/s)$

$Q = applied\ flow\ rate\ (m^3/s)$

$A_h = the\ horizontal\ area\ of\ the\ unit\ (m^2)$

(10)

$$U = 25V^{1/6}$$

$V = volume\ of\ the\ bubble$

(11)

$$\frac{1}{2}C_D S\rho U^2 = \Delta\rho g V$$

$C_D = the\ drag\ coefficient$

$S = \pi d_e^3/6$

(12)

$$C_D = \frac{4g\Delta\rho d_e^3}{3\rho d_h^2 U^2}$$

(13)

$$U = (\frac{8gV}{\pi C_D d_h^2})^{\frac{1}{2}}$$

$$U = (\frac{8g}{6^{2/3}\pi^{1/3}C_D})^{1/2} V^{1/6} \frac{d_e}{d_h}$$

$$C_D = \frac{24(1+0173Re^{0.657})}{Re} + \frac{0.413}{1+16300Re^{-1.09}}$$

$for\ Re < 1,\ C_D = 24/Re\ and\ d_e/d_h = 1 = 1$

Table 9: Bubble size relationship in between, rise velocity, temperature, and laminar flow(P.1988)

Bubble Size (μm)	Rise Velocity (m/h) Above Which Turbulent Flow Exists[a]		Terminal Rise Velocity (m/h) Based on Stokes' Law	
	4°C	20°C	4°C	20°C
10	565	360	0.125	0.196
20	283	180	0.499	0.783
30	188	120	1.12	1.76
40	141	90	2.00	3.13
50	113	72	3.12	4.89
80	70.7	45	7.99	12.5
110	51.4	32.7	15.1	23.7
120	47.1	30	18.0	28.2
130	43.5	27.7	21.1	33.1[b]
140	40.4	25.7	24.5	38.3[b]
160	35.3	22.5	31.9	50.1[b]
170	33.2	21.2	36.1[b]	56.5[b]

Aerobic digester

The idea behind all contemporary high rate biomethanation techniques is to immobilize bacterial sludge in some way in order to retain high viable biomass. One of the following techniques is used to accomplish these (Pol & Lettinga 1986):

(Rajeshwari et al. 2000) found that anaerobic baffled reactors and upflow anaerobic sludge blanket reactors are examples of systems that combine the formation of highly settleable sludge aggregates with gas separation and sludge settling. adhesion of bacteria to high density particle carrier materials, such in anaerobic expanded bed reactors and fluidized bed reactors. Sludge aggregates become trapped between packing materials that are provided to the reactor, such as upflow and downflow anaerobic filters.

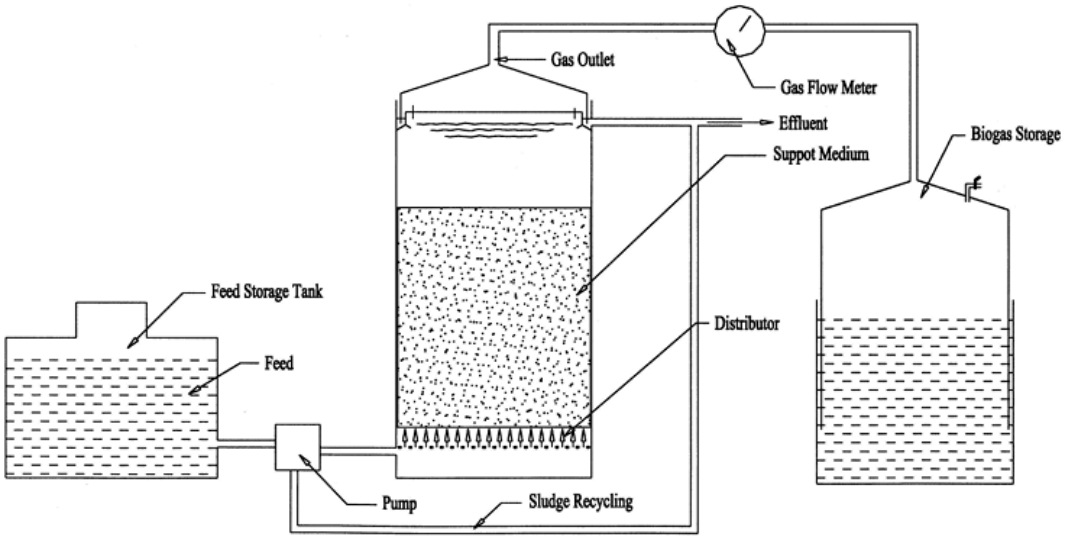

Figure 29: Fixed film digester.

The sludge can be evacuated through centrifugal techniques, a vacuum, a press, a horizontal band filter, a bore press, drying beds, and sludge lagoons. At the same time (Demirbas et al. 2017) mentioned a few systems like vacuum, press, and horizontal band filters are expensive to invest in and run, need specialized personnel, and require apparatus and equipment.

After sludge dewatering, increasing the dry matter content from 20–25% to 90% results in a significant reduction in sludge mass. Energy is required for the drying process in order to dewater. 2,500 kJ/kg of water is the energy needed to evaporate it. This number is considered to be between 2,750 and 3,100 kJ/kg of water when heat losses are taken into account. The energy contents (MJ/kg) and organic dry matter contents (%) of dried sewage sludge and crude sludge are 8.4–11.5, 12.6–18.4, and 60–80, respectively (Fytili & Zabaniotou 2008).

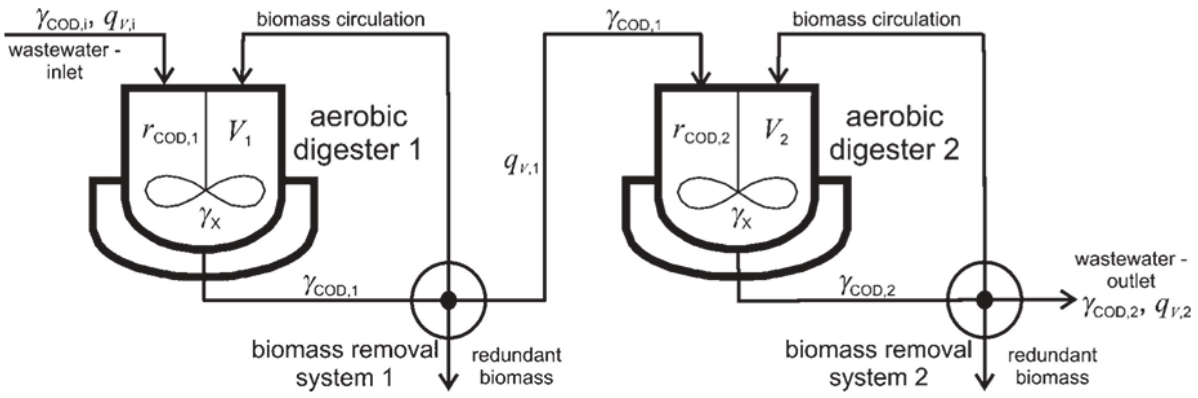

Figure 30: Two anaerobic digesters connected in series that are not equal(Goršek 2007)

Typically, the aeration basin (digester) is treated as a perfectly mixed vessel, and anaerobic sludge is viewed as a single pseudo-species with a growth rate that follows assumed dynamics. If we assume equal inlet and exit industrial wastewater volume flow rates (qV,i =qV,1=qV,2=qV), then the degradation rate of OM expressed as COD, using the CSTR model under steady-state circumstances, may be given independently for anaerobic digester1, by equation:

$$-r_{COD,1} = \frac{1}{Y_{X/COD}}\mu\gamma_X = \frac{q_V}{V_1}(\gamma_{COD,i} - \gamma_{COD,1})$$

(Bailey & Ollis 2018)

For aerobic digester 1

$-r_{COD,1}$ = degradation rate of organic compounds (OM) in aerobic digester 1, $Kg\ m^{-3}d^{-1}$

V_1 = volume of aerobic digester 1

μ = specific growth rate of biomass, d^{-1}

$Y_{X/COD}$ = Yield biomass degrading (OM), $Kg\ Kg^{-1}$

$\gamma_{COD,i}$ = inlet mass concentration of OM, $kg\ m^{-3}$

$\gamma_{COD,1}$ = outlet mass concentration of OM from digester 1, $kg\ m$

$$-r_{COD,2} = \frac{1}{Y_{x/COD}}\mu\gamma_X = \frac{q_v}{V_2}(\gamma_{COD,1} - \gamma_{COD,2})$$

(Burhan et al. 2005)

For aerobic digester 2

$-r_{COD,2}$ = degradation rate of organic compounds (OM) in aerobic digester 2, $Kg\ m^{-3}d^{-1}$

V_2 = volume of aerobic digester 2

γ_X = mass concentration biomass, $Kg\ m^{-3}$

$\gamma_{COD,2}$ = outlet mass concentration of OM from digester 2, $kg\ m$

$$\mu = \frac{\mu_{max}\gamma_{COD}}{K_s+\lambda_{COD}} exp(-\frac{\gamma_{COD}}{K_{IA}})$$

(Aiba et al. 1968)

$\mu_{max} = maximum\ specific\ growth\ rate\ of\ biomass, d^{-1}$

$K_s = saturation\ constant\ of\ OM,\ kg\ m^{-3}$

$K_{IA} = Aiba's\ inhibition\ coefficient,\ Kg\ m^{-3}$

$Y_{X/COD} = Total\ OM\ concentration$

$$-r_{COD,1} = \frac{r_{max}\gamma_{COD,1}}{K_s+\gamma_{COD,1}} exp(-\frac{\gamma_{COD,1}}{K_{IA}}) = \frac{q_v}{V_1}(\gamma_{COD,i} - \gamma_{COD,1}$$

Additionally, regardless of qV, which is attained with biomass circulation, X in both digesters remains constant.Given equation (3) and the aforementioned presumptions, equations (1) and (2) can be defined as follows:

$$-r_{COD,2} = \frac{r_{max}\gamma_{COD,2}}{K_s+\gamma_{COD,2}} exp(-\frac{\gamma_{COD,2}}{K_{IA}}) = \frac{q_v}{V_2}(\gamma_{COD,1} - \gamma_{COD,2}$$

$$V_1 = (\frac{r_{max}\gamma_{COD,1}}{k_s+\gamma_{COD,1}} exp(-\frac{\gamma_{COD,1}}{K_{IA}}))^{-1}.q_v(\gamma_{COD,1} - \gamma_{COD,1})$$

$r_{max} = maximum\ degradation\ of\ OM,\ kg\ m^{-3}d^{-1}$

$$V_2 = (\frac{r_{max}\gamma_{COD,2}}{k_s+\gamma_{COD,2}} exp(-\frac{\gamma_{COD,2}}{K_{IA}}))^{-1}.q_v(\gamma_{COD,1} - \gamma_{COD,2})$$

$$\frac{dr_{COD}}{d\gamma_{COD}} = (\frac{r_{max}}{K_s+\gamma_{COD}} - \frac{r_{max}\gamma_{COD}}{(K_s+\gamma_{COD})^2} - \frac{r_{max}\gamma_{COD}}{(K_s+\gamma_{COD})K_{IA}}) exp(-\frac{\gamma_{COD}}{K_{IA}}) = 0$$ (Livenspiel 1972)

Typically, the curve-rCOD=f(COD) has a certain convex form when OM inhibition is present.Consequently, the curve's maximum follows the equation, adopting Aiba's formulation.

(10) $$\eta_{COD} = \frac{\gamma_{COD,i} - \gamma_{COD}}{\gamma_{COD,i}}.100$$

Table 1 lists the measured outlet mass concentrations of OM and COD at various industrial wastewater volume flow rates, qV, under steady-state circumstances. Confidence intervals (CF), corresponding dilution rates (D), OM and COD degradation rates, and wastewater treatment efficiencies (COD) were computed. The difference between COD,i = (5.10 0.10) kg m–3 and COD is multiplied by D to get the –rCOD. Additionally, the following formula was used to determine the COD:

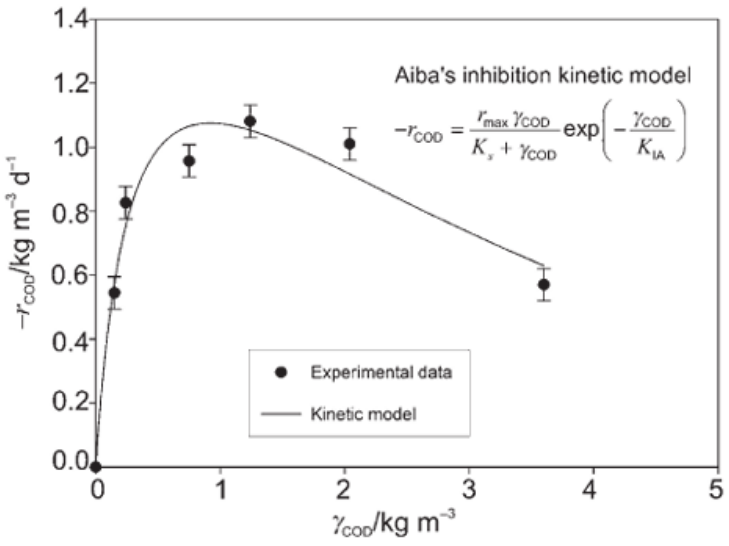

Figure 31: Model Base values of degradation of OM (Goršek 2007).

Over 97% of the organic matter (OM) found in the industrial wastewater at D = 0.11 d^{-1} was eliminated by the aerobic biomass sludge (see Table10 6′s sixth column). Additionally, the mass fraction of plant tannins with respect to overall outflow remained nearly the same as that with reference to inflow (W_T = 30%), as demonstrated by the UV spectrophotometric method18 for chemical analysis of tannins. Thus, it can be said that the biomass sludge from the current wastewater treatment plant has a good capacity to break down plant tannins in industrial wastewater. However, as the dilution rate increases, the wastewater treatment efficiency drops off significantly. At D = 0.28 d^{-1}, where the wastewater efficiency was only 76%, the maximum rate of OM degradation was attained.

q_V/m^3 d^{-1}	D/d^{-1}	γ_{COD}/kg m^{-3}	$-r_{COD}$/kg m^{-3} d^{-1}	CF/%	η_{COD}/%
0.0010	0.11 ± 0.01	0.150 ± 0.02	0.544 ± 0.051	9.3	97.1 ± 2.8
0.0015	0.17 ± 0.01	0.240 ± 0.02	0.826 ± 0.052	6.2	95.3 ± 2.7
0.0020	0.22 ± 0.01	0.750 ± 0.06	0.957 ± 0.050	5.3	85.3 ± 2.8
0.0025	0.28 ± 0.01	1.240 ± 0.06	1.081 ± 0.051	4.7	76.7 ± 2.7
0.0030	0.33 ± 0.01	2.040 ± 0.07	1.010 ± 0.051	5.0	60.0 ± 2.7
0.0035	0.38 ± 0.01	3.600 ± 0.08	0.570 ± 0.051	8.9	29.4 ± 2.6

(Goršek 2007) demonstrated that the mass balance of OM data from studies in the laboratory bench-top aerobic digester was effectively used to calculate the kinetic parameters of the Aiba′s inhibitory kinetic model. Then, using the criterion of a minimal total holding time, we calculated the ideal volumes of two aerobic digesters connected in series. Industrial wastewater volume flow rate (qV = 120 m3 d–1) and wastewater treatment efficiency (COD = 98%) served as the basis for the evaluation. Two aerobic digesters with V1 = 467 m3 and V2 = 228 m3 were produced

under these circumstances. A two-stage industrial wastewater treatment facility's technological and financial approval was primarily validated by the fact that its total digester volume was more than twice that of a one-stage plant. As a result, it was demonstrated how crucial it is to build aerobic digesters based on the minimal holding duration of two digesters connected in series.

Centrifuge and sludge thickening:

Types of centrifuges

In municipal wastewater treatment plants it is best to use typical automated handling of biosolids through sedimentation type centrifuges, as listed in the following table 10.

Table 10: Different types of centrifuges employed in municipal waste water treatment plants(Wang et al. 2024).

Type centrifuge	Particle size	Maximum centrifugal force $Level\ x\ G$	Feed concentration %	Capacity range m^3/hr (GMP)	Solids Discharge	Manner of solids discharge
Scroll-solid bowl	$6400\mu\ to\ > 1\mu$	$3,000$	$1 - 50$	$\frac{1}{4} - 250$ $(1 - 1000)$	Solid	Continuous
Disc-Nozzle	$100\mu\ to\ > 1\mu$	$4,000$	$2 - 10$	$\frac{1}{4} - 250$ $(1 - 1000)$	Fluid	Continuous
Disc-valve opening	$100\mu\ to\ > 1\mu$	$4,000$	$2 - 10$	$\frac{1}{4} - 180$ $(1 - 800)$	Fluid	Controlled Cycle

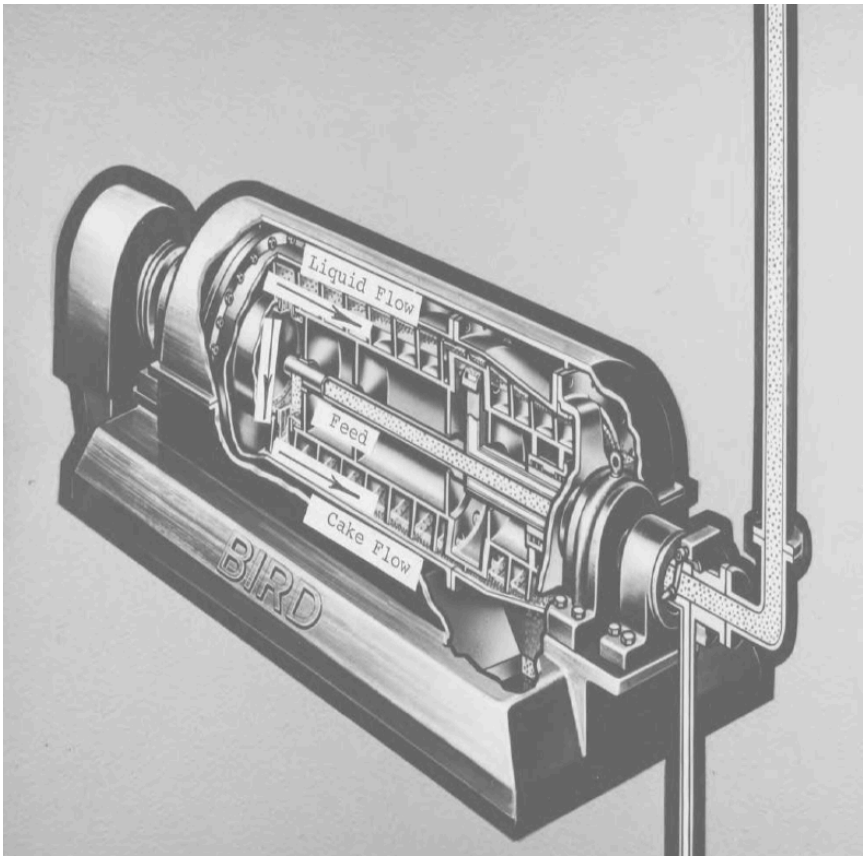

Figure 31: Centrifugal apparatus

The centrifugal apparatus is demonstrated in figure 31 by the following equipment, which pumps the solid waste intake into the centrifuge machine. The liquids collected at the outer chamber are fed back into the aerobic digester, leaving the dry solids suitable for transportation to a landfill. The centrifugal apparatus is made to rotate at a high speed in order to dewater the liquid from the particles.

Conclusion

This study examined the effects of primary treatment techniques (primary clarifier, A stage, or CEPT) on the digestibility and properties of sludge as well as the economics of the entire plant. The digestibility and properties of the sludge were significantly impacted by the treatment procedure and technology. Digestion of primary sludge produced the maximum quantity of methane, followed by A-sludge. Primary sludge included the highest amount of lipids, cellulose and hemicellulose, while A-sludge had the highest amounts of proteins and CEPT sludge had the highest amounts of lignin. According to plant-wide mass balances, the amount of organic matter in wastewater converted into methane gas was approximately 20, 27.4, and 33.4% with the implementation of primary clarifier, A-stage, and CEPT, respectively. CEPT sludge digestion yielded the lowest amount of methane, which was 30% lower than that of primary sludge.

Due to space, odour, and sludge limits, integrated anaerobic-aerobic bioreactors have gained popularity for combining aerobic and anaerobic processes in one unit.

Compact integrated bioreactors are expected to be able to treat a variety of high organic strength industrial and municipal wastewater due to its straightforward yet affordable technology, ability to generate renewable energy, and exceptional treatment efficiency. However, the majority of the integrated bioreactors described in this paper have not been widely implemented in industry, and more research is necessary to assess these promising reactors′ performance on a larger scale. Additionally, it is seen to be crucial to make other advancements like installing a biogas capture system and using packing medium or suspended carriers.

This research highlights the potential for significant cost reductions and improved efficiency in wastewater treatment through the integration of membrane technologies. The findings suggest that combining reverse osmosis, forward osmosis, and nanofiltration could lead to substantial improvements in both water recovery and contaminant removal from pharmaceutical wastewaters. However, further economic analysis is needed to determine the feasibility of implementing these technologies on an industrial scale.

This report is a research project that has been prepared on behalf of Ahmad Samadi in accordance with the terms and conditions of Building & Infrastructure Pty Ltd (ACN 669 776 845). Engineering Building & Infrastructure cannot be held responsible for any use of, or reliance on its contents by any third party.

The comments and recommendations in this report are derived from our visual observations and our analytical expertise in dealing with similar matters previously. Unless stated otherwise, no invasive enquiries were conducted.

References

Abdelrahman, A.M. et al., 2023. Impact of primary treatment methods on sludge characteristics and digestibility, and wastewater treatment plant-wide economics. *Water research*, 235(119920), p.119920.

Adlan, M.N.B., 1998. *A study of dissolved air flotation tank design variables and separation zone performance*. Degree of Doctor of Philosophy in Environmental Engineering. Malasia: Degree of Doctor of Philosophy in Environmental Engineering. Available at: http://theses.ncl.ac.uk/jspui/handle/10443/409.

Aggelis, G.G., Gavala, H.N. & Lyberatos, G., 2001. Combined, separate aerobic and anaerobic biotreatment of green olive debittering wastewater. *Journal of Agricultural Engineering Research*, 80, pp.283–292.

Aiba, S., Shoda, M. & Nagatani, M., 1968. Kinetics of product inhibition in alcohol fermentation. *Biotechnology and bioengineering*, 10(6), pp.845–864.

American Water Works Association, 2011. *M37 operational control of coagulation and filtration processes, third edition*, American Water Works Association.

Amirtharajah, A., 1988. Some theoretical and conceptual views of filtration. *Journal - American Water Works Association*, 80(12), pp.36–46.

Anon, 2016. Grit Removal Systems. *Sewage Treatment - Reverse Osmosis - Waste water Treatment*. Available at: https://www.aesarabia.com/grit-removal-systems/ [Accessed October 21, 2024].

Anon, Products and equipment for your individual needs. Available at: https://www.huber-se.com/products/ [Accessed October 21, 2024a].

Anon, » Vortex Grit Removal Systems. Available at: https://napier-reid.com/products/vortex-grit-removal-systems/ [Accessed October 21, 2024b].

Astals, S. et al., 2014. Identification of synergistic impacts during anaerobic co-digestion of organic wastes. *Bioresource technology*, 169, pp.421–427.

Bailey, J.E. & Ollis, D.F., 2018. Biochemical engineering fundamentals. Available at: https://modps71.lib.kmutt.ac.th/xmlui/handle/123456789/324.

Belford, I., 2013. Investigating the removal of Candida and other potential pathogens from wastewater via an experimental rhizofiltration system. Available at: https://scholar.sun.ac.za/handle/10019.1/79806.

Bellar, T.A., Lichtenberg, J.J. & Kroner, R.C., 1974. The occurrence of organohalides in chlorinated drinking waters. *Journal - American Water Works Association*, 66(12), pp.703–706.

Burhan, N., Sapundzhiev, T. & Beschkov, V., 2005. Mathematical modelling of cyclodextrin-glucanotransferase production by batch cultivation. *Biochemical engineering journal*, 24(1), pp.73–77.

Cakir, F.Y. & Stenstrom, M.K., 2005. Greenhouse gas production: a comparison between aerobic and anaerobic wastewater treatment technology. *Water research*, 39(17), pp.4197–4203.

Calderon, R.L., 2000. The epidemiology of chemical contaminants of drinking water. *Food and chemical toxicology: an international journal published for the British Industrial Biological Research Association*, 38(1 Suppl), pp.S13–20.

Caltrans Division of Design, 2020. Flow Splitters. In *Design Guidance for flow splitters*. California Department of Transportation HQ Division of Design.

Camp, T.R., 1946. Sedimentation and the design of settling tanks. *Transactions of the American Society of Civil Engineers*, 111(1), pp.895–936.

Cervantes, F.J., Pavlostathis, S.G. & van Haandel, A., 2006. *Advanced biological treatment processes for industrial wastewaters* F. J. Cervantes, S. G. Pavlostathis, & A. C. van Haandel, eds., London, England: IWA

Publishing.

Charles R. O'Melia, M.A., Particles, pretreatment, and performance in water filtration. , (1985). Available at: https://ascelibrary.org/doi/abs/10.1061/(ASCE)0733-9372(1985)111:6(874).

Cheremisinoff, P.N., 2019. *Handbook of water and wastewater treatment technology*, Routledge.

Chien, M.H., Borys, A. & Wong, J.L., 2010. Computational fluid dynamics analysis of a vortex grit removal system. In *WEFTEC 2010*. Water Environment Federation, pp. 6020–6032.

Cho, H. & Sansalone, J., 2013. Physical modeling of particulate matter washout from a hydrodynamic separator. *Journal of environmental engineering (New York, N.Y.)*, 139(1), pp.11–22.

Coats, E.R. & Wilson, P.I., 2017. Toward nucleating the concept of the water resource recovery facility (WRRF): Perspective from the principal actors. *Environmental science & technology*, 51(8), pp.4158–4164.

Demirbas, A. et al., 2017. Aerobic digestion of sewage sludge for waste treatment. *Energy Sources Part A Recovery Utilization and Environmental Effects*, 39(10), pp.1056–1062.

Droste, R.L. & Gehr, R.L., 2018. *Theory and practice of water and wastewater treatment* 2nd ed., Nashville, TN: John Wiley & Sons.

Duong, H.A. et al., 2003. Trihalomethane formation by chlorination of ammonium- and bromide-containing groundwater in water supplies of Hanoi, Vietnam. *Water research*, 37(13), pp.3242–3252.

Fukushi, K., Tambo, N. & Matsui, Y., 1995. A kinetic model for dissolved air flotation in water and wastewater treatment. *Water science and technology: a journal of the International Association on Water Pollution Research*. Available at: https://www.sciencedirect.com/science/article/pii/027312239500202X.

Fytili, D. & Zabaniotou, A., 2008. Utilization of sewage sludge in EU application of old and new methods—A review. *Renewable and Sustainable Energy Reviews*, 12(1), pp.116–140.

Ge, H. et al., 2017. Nutrient removal and energy recovery from high-rate activated sludge processes - Impact of sludge age. *Bioresource technology*, 245(Pt A), pp.1155–1161.

Goršek, M.T.A., 2007. Aerobic digester design for the biodegradation of plant tannins in industrial wastewater.

Graef, S.P. & Andrews, J.F., 1974. Mathematical modeling and control of anaerobic digestion. *Water research*.

Gray, N.F., 2010. *Water technology: An introduction for environmental scientists and engineers* 3rd ed., Taylor & Francis Group.

Harper, J.F., 1972. The motion of bubbles and drops through liquids. *Advances in applied mechanics*. Available at: https://www.sciencedirect.com/science/article/pii/S0065215608701339.

Heijnen, J.J. et al., 1991. Large scale anaerobic-aerobic treatment of complex industrial waste water using biofilm reactors. *Water science and technology: a journal of the International Association on Water Pollution Research*, 23(7-9), pp.1427–1436.

Horio, M. et al., 2009. Development of biomass charcoal combustion heater for household utilization. *Industrial & engineering chemistry research*, 48(1), pp.361–372.

Incropera, F.P. & DeWitt, D.P., 1990. *Introduction to heat transfer*, Brisbane, QLD, Australia: John Wiley and Sons (WIE).

Ison, C.R. & Ives, K.J., 1969. Removal mechanisms in deep bed filtration. *Chemical engineering science*, 24(4), pp.717–729.

Jameson, G.J., 1984. Experimental Techniques in Flotation. In *The Scientific Basis of Flotation*. Dordrecht: Springer Netherlands, pp. 193–228.

Joe Middlebrooks, E. et al., Nitrogen Removal in Wastewater Stabilization Lagoons. Available at: https://www.researchgate.net/profile/Vd-Adams/publication/238695616_Nitrogen_Removal_in_Wastewater_Stabilization_Lagoons/links/56aa27b508ae7f592f0f21ce/Nitrogen-Removal-in-Wastewater-Stabilization-Lagoons.pdf.

Kafle, G.K. & Chen, L., 2016. Comparison on batch anaerobic digestion of five different livestock manures and prediction of biochemical methane potential (BMP) using different statistical models. *Waste management (New York, N.Y.)*, 48, pp.492–502.

Kawamura, S. & McGivney, W.T., 2007. *Cost estimating manual for water treatment facilities: McGivney/cost estimating manual*, Nashville, TN: John Wiley & Sons.

Leslie Grady, C.P. et al., 2009. *Biological wastewater treatment, third edition* 3rd ed., Boca Raton, FL: CRC Press. Available at: https://books.google.com/books?hl=en&lr=&id=stjLBQAAQBAJ&oi=fnd&pg=PP1&dq=C.P.+Leslie+Grady+Jr.,+G.T.+Daigger,+H.C.+Lim,+Biological+Wastewater+Treatment,+second+ed.,+revised+and+expanded,+CRC+Press,+1999.&ots=r-aQGBenG8&sig=iMrXn2_AP4cZErb1U1bJhX55xb8.

Lindeburg, M.R., 2005. *Civil PE exam structural code supplement for the civil engineering reference manual, ninth ition*, Professional Publications.

Lindeburg, M.R., 1999. *Practice problems for the civil engineering PE exam* 7th ed., Professional Publications.

Livenspiel, O., 1972. Chemical reaction engineering.

Li, W.S. & Lam, S.H., 1964. Principles of fluid me-chanics. Addison and Wesley. *Reading, Massa-chusetts*.

Logsdon, G.S. et al., 2006. Filtration processes-A distinguished history and a promising future. *Journal - American Water Works Association*, 98(3), pp.150–162.

Lund, V. 62: 171–177, Micro screening in wastewater treatMent – an overview. Available at: https://www.tidskriftenvatten.se/wp-content/uploads/2017/04/48_article_2139.pdf.

Mazhar, M.A. et al., 2020. Chlorination disinfection by-products in municipal drinking water – A review. *Journal of cleaner production*, 273(123159), p.123159.

Metcalf, L., Eddy, H.P. & Tchobanoglous, G., 1991. Wastewater engineering: treatment, disposal, and reuse. , 4. Available at: https://library.wur.nl/WebQuery/titel/1979505.

Middlebrooks, E.J. & Pano, A., 1983. Nitrogen removal in aerated lagoons. *Water research*, 17(10), pp.1369–1378.

Narayanan, C.M., 2011. Biotechnology and bioprocess engineering.

Narayanan, C.M., 1993. Energy conservation employing membrane-based technology. *Chemical Industry Digest*, 6(1), pp.133–136.

Narayanan, C.M., 2012. Production of phosphate-rich biofertiliser using vermicompost and anaerobic digestor sludge—a case study. Available at: https://www.scirp.org/html/1-3700153_18876.htm.

Narayan, V., Vinod, J.K. & Kumar, S., 2005. Cultivation of Recombinant E. Coli using LPO Strategy. In *Proc. Chemical Eng. Congress, New Delhi*.

O'Melia, C.R. & Ali, W., 1979. The role of retained particles in deep bed filtration. In S. H. Jenkins, ed. *Ninth International Conference on Water Pollution Research*. Elsevier, pp. 167–182.

Operator, T.P., 2019. A Grit Removal System From HUBER Technology Does Double Duty. *Treatment Plant Operator*. Available at: https://www.tpomag.com/editorial/2019/03/a-grit-removal-system-from-huber-technology-does-double-duty [Accessed October 21, 2024].

Packham, R.F. & Richards, W.N., 1972. Water Clarification by Flotation 1: A Survey of the Literature. *WRA Tech. Paper TP87, Medmenham*.

PK Swamee, C.O., 1991. Bed-load and suspended-load transport of nonuniform sediments. Available at: https://ascelibrary.org/doi/abs/10.1061/(ASCE)0733-9429(1991)117:6(774).

P., M.J.J., 1988. A fundamental study of dissolved air flotation for treatment of low turbidity waters containing natural organic matter. Available at: https://search.proquest.com/openview/30f991a1bab1e7b25a343b447f6ba252/1?pq-origsite=gscholar&cbl=18750&diss=y.

Pol, L.H. & Lettinga, G., 1986. New technologies for anaerobic wastewater treatment. *Water Science and technology*, 18(12), pp.41–53.

Pretorius, C.F., 2012. A review of vortex grit basin design. *Proceedings of the Water Environment Federation*, 2012(10), pp.5715–5734.

Rahman, A. et al., 2019. A-stage and high-rate contact-stabilization performance comparison for carbon and nutrient redirection from high-strength municipal wastewater. *Chemical engineering journal (Lausanne, Switzerland: 1996)*, 357, pp.737–749.

Rajagopalan, R. & Tien, C., 1977. Single collector analysis of collection mechanisms in water filtration. *The Canadian journal of chemical engineering*, 55(3), pp.246–255.

Rajeshwari, K.V. et al., 2000. State-of-the-art of anaerobic digestion technology for industrial wastewater treatment. *Renewable and Sustainable Energy Reviews*, 4(2), pp.135–156.

Rao, K.R. & Subrahmanyam, N., 2004. Process variations in activated sludge process–a review. *Ind Chem Engr*, 46, pp.48–55.

Ratnayaka, D.D., 2009. *Water Supply* 6th ed., Woburn, MA: Butterworth-Heinemann. Available at: https://books.google.com/books?hl=en&lr=&id=XTrvVSJTnUEC&oi=fnd&pg=PP1&dq=Ratnayaka,+D.D.%3B+Brandt,+M.J.%3B+Johnson,+K.M.+Twort%E2%80%99s+Water+Supply,+6th+ed.%3B+Butterworth-Heinemann:+Oxford,+MA,+USA,+2009.&ots=QZi7zgTifE&sig=drUdo0LmLD6Py6Gt1j4YsiKx07M.

Reid, G.W. & Streebin, L., 1979. *Performance evaluation of existing aerated lagoon system at*, Bixby, Oklahoma; Cincinnati, OH.

Repo, M.A. et al., 1988. Effect of gallium on bone mineral properties. *Calcified tissue international*, 43(5), pp.300–306.

Richardson, J.F., Harker, J.H. & Backhurst, J.R., 2014. *Chemical Engineering Volume 2* 5th ed., Woburn, MA: Butterworth-Heinemann. Available at: https://books.google.com/books?hl=en&lr=&id=ottGCe1CDUoC&oi=fnd&pg=PP1&dq=Coulson,+J.M.,+J.F.+Richardson,+J.R.+Backhurst+and+J.H.+Harker+(1991)+Chemical+Engineering,++Volume+2,+4th+edition,+The+Bath+Press,+Bath,+Great+Britain&ots=BlLQXZb0Lw&sig=jpzeaJjlRPUeUU0a93s-UXzDVI4.

Rook, J.J., 1972. Formation of haloform during chlorination of natural water. *Water Treatment and Examination*, 21, p.259.

Rouse, H., 1937. Modern conceptions of the mechanics of fluid turbulence. *Transactions of the American Society of Civil Engineers*, 102(1), pp.463–505.

Ruyack, A.R., 2019. Alkali Metal-Based Transient Microsystems and Near-Zero Power Radio Receivers. Available at: https://search.proquest.com/openview/6827660fc4a9517cc24af4f043af55b5/1?pq-origsite=gscholar&cbl=18750&diss=y.

Scherson, Y.D. & Criddle, C.S., 2014. Recovery of freshwater from wastewater: upgrading process configurations to maximize energy recovery and minimize residuals. *Environmental science & technology*, 48(15), pp.8420–8432.

Schmidt, J., Seto, P. & Averill, D., 1997. Pilot-scale study of satellite treatment options for the control of combined sewer overflows. *Water Quality Research Journal*, 32(1), pp.169–184.

Sekhar, D.M.R., Principles of phosphate fertilization and PROM–progress review 2012. *researchgate.net*. Available at: https://www.researchgate.net/profile/Dmr-Sekhar/publication/235918492_Principles_of_Phosphate_Fertilization_and_PROM_-_Progress_Review_2012/links/0046351425b840540c000000/Principles-of-Phosphate-Fertilization-and-PROM-Progress-Review-2012.pdf.

Slavik, I., Jehmlich, A. & Uhl, W., 2013. Impact of backwashing procedures on deep bed filtration productivity in

drinking water treatment. *Water research*, 47(16), pp.6348–6357.

Smith, R., 1970. USEPA report: 170–40–05–70.

Spellman, F.R., 2008. *Handbook of water and wastewater treatment plant operations, second edition* 2nd ed., Boca Raton, FL: CRC Press. Available at: https://www.taylorfrancis.com/books/mono/10.1201/9781420075311/handbook-water-wastewater-treatment-plant-operations-frank-spellman.

Stephenson, T. et al., 2000. *Membrane Bioreactors for Wastewater Treatment*, London, England: IWA Publishing.

Steven J. Wright, Daniel B. Schlapfer, Razik Al-Saigh, 1988. *Hydraulic model study wastewaterinfluent splitter chamber*. Final Project Report. United States, Michigan: THE UNIVERSITY OF MICHIGAN DEPARTMENT OF CIVIL ENGINEERING ANNARBOR, MICHIGAN. Available at: https://deepblue.lib.umich.edu/bitstream/handle/2027.42/154194/39015101405192.pdf?sequence=1.

Stratton, F.E., 1969. Nitrogen losses from alkaline water impoundments. *Journal of the Sanitary Engineering Division*, 95(2), pp.223–232.

Stuetz, R.M. & Stephenson, T., 2009. *Principles of water and wastewater treatment processes* R. M. Stuetz & T. Stephenson, eds., London, England: IWA Publishing.

Sullivan, R.H., National Environmental Research Center (Cincinnati, Ohio) & American Public Works Association, 1974. *The swirl concentrator as a grit separator device*, U.S. Environmental Protection Agency, Office of Research and Development, National Environmental Research Center.

Swamee, P.K. & Tyagi, A., 1996. Design of class-I sedimentation tanks. *Journal of environmental engineering*. Available at: https://ascelibrary.org/doi/abs/10.1061/(ASCE)0733-9372(1996)122:1(71).

Tebbutt, T.H.Y., 1997. *Principles of Water Quality Control*, Elsevier.

Thakura, R., Chakrabortty, S. & Pal, P., 2015. Treating complex industrial wastewater in a new membrane-integrated closed loop system for recovery and reuse. *Clean technologies and environmental policy*, 17(8), pp.2299–2310.

Thokchom, B., Radhapyari, K. & Dutta, S., 2020. Occurrence of trihalomethanes in drinking water of Indian states: a critical review. In M. N. V. Prasad, ed. *Disinfection By-products in Drinking Water*. Elsevier, pp. 83–107.

Tsai, W.T. et al., 2006. Characterization and adsorption properties of eggshells and eggshell membrane. *Bioresource technology*, 97(3), pp.488–493.

Twort, A.C., Ratnayaka, D.D. & Brandt, M.J., 2000. *Water Supply* 5th ed., Woburn, MA: Butterworth-Heinemann. Available at: https://books.google.com/books?hl=en&lr=&id=wjl_7A8ZMeIC&oi=fnd&pg=PP2&dq=Twort,+A.C.%3B+Ratnayaka,+D.D.%3B+Brandt,+M.J.+Water+Supply,+3rd+ed.%3B+Butterworth-Heinemann:+Oxford,+MA,+USA,+2000.&ots=y7Q1rYCiyY&sig=E3YFD4ePVATFM9kTerqK1sthg7M.

Vera, M. et al., 1999. Optimization of a sequential anaerobic-aerobic treatment of a saline fishing effluent. *Process safety and environmental protection : transactions of the Institution of Chemical Engineers, Part B*, 77(5), pp.275–290.

Wang, L.K. et al. eds., 2005. *Waste treatment in the process industries*, Boca Raton, FL: CRC Press. Available at: https://www.taylorfrancis.com/books/mono/10.1201/9781420037159/waste-treatment-process-industries-howard-lo-yung-tse-hung-constantine-yapijakis-lawrence-wang.

Wang, L.K., Wang, M.-H.S. & White, W.F., 2024. CENTRIFUGATION ENGINEERING. Available at: http://dx.doi.org/10.17613/b61f-1688.

White, F.M., 1994. Fluid mechanics., Editorial McGraw Hill. *Inc. New York*.

Wilson, G., Tchobanoglous, G. & Griffiths, J., 2007. OPERATIONS FORUM-A SPECIAL SECTION FOR OPERATORS-The Nitty Gritty-Grit washing system design. *Water Environment and Technology*, 19(10), pp.81–84.

Zabot, G.L. et al., 2011. Hybrid modeling of xanthan gum bioproduction in batch bioreactor. *Bioprocess and biosystems engineering*, 34(8), pp.975–986.

Zamani, A. & Maini, B., 2009. Flow of dispersed particles through porous media — Deep bed filtration. *Journal of petroleum science & engineering*, 69(1-2), pp.71–88.

Zouboulis, A., Traskas, G. & Samaras, P., 2007. Comparison of single and dual media filtration in a full-scale drinking water treatment plant. *Desalination*, 213(1-3), pp.334–342.